



UWS Academic Portal

U-Pb zircon age dating of diamond-bearing gneiss from Fjørtoft reveals repeated burial of the Baltoscandian margin during the Caledonian Orogen

Walczak, Katarzyna; Cuthbert, Simon; Kooijman, Ellen Kooijman; Majka, Jaroslav; Smit, Matthias

Published in:
Geological Magazine

DOI:
[10.1017/S0016756819000268](https://doi.org/10.1017/S0016756819000268)

Published: 30/11/2019

Document Version
Peer reviewed version

[Link to publication on the UWS Academic Portal](#)

Citation for published version (APA):

Walczak, K., Cuthbert, S., Kooijman, E. K., Majka, J., & Smit, M. (2019). U-Pb zircon age dating of diamond-bearing gneiss from Fjørtoft reveals repeated burial of the Baltoscandian margin during the Caledonian Orogen. *Geological Magazine*, 156(11), 1949-1964. [GEO-18-2102.R2]. <https://doi.org/10.1017/S0016756819000268>

General rights

Copyright and moral rights for the publications made accessible in the UWS Academic Portal are retained by the authors and/or other copyright owners and it is a condition of accessing publications that users recognise and abide by the legal requirements associated with these rights.

Take down policy

If you believe that this document breaches copyright please contact pure@uws.ac.uk providing details, and we will remove access to the work immediately and investigate your claim.

U-Pb zircon age dating of diamond-bearing gneiss from Fjørtoft reveals repeated burial of the Baltoscandian margin during the Caledonian Orogeny

Journal:	<i>Geological Magazine</i>
Manuscript ID	GEO-18-2102.R2
Manuscript Type:	Original Article
Date Submitted by the Author:	19-Feb-2019
Complete List of Authors:	Walczak, Katarzyna; AGH University of Science and Technology , Faculty of Geology, Geophysics and Environmental Protection Cuthbert, Simon; School of Computing, Engineering & Physical Sciences, University of the West of Scotland, Paisley, United Kingdom Kooijman, Ellen; Swedish Museum of Natural History, Department of Geosciences Majka, Jaroslaw; Uppsala University, Department of Earth Sciences; AGH University of Science and Technology , Faculty of Geology, Geophysics and Environmental Protection Smit, Matthijs; University of British Columbia, Department of Earth, Ocean and Atmospheric Sciences
Keywords:	geochronology, Western Gneiss Region, ultrahigh pressure metamorphism, U-Pb zircon dating

1
2
3 **1 U-Pb zircon age dating of diamond-bearing gneiss from Fjørtoft reveals repeated**
4
5 **2 burial of the Baltoscandian margin during the Caledonian Orogeny**
6
7

8 3

9
10 4 Katarzyna Walczak¹, Simon Cuthbert², Ellen Kooijman³, Jarosław Majka^{1,4}, Matthijs A.
11
12 5 Smit⁵
13

14 6

15
16
17 7 ¹ Faculty of Geology, Geophysics and Environmental Protection, AGH University of
18
19 8 Science and Technology, Kraków, Poland

20
21 9 ² School of Computing, Engineering & Physical Sciences, University of the West of
22
23 10 Scotland, Paisley, United Kingdom

24
25
26 11 ³ Department of Geosciences, Swedish Museum of Natural History, Stockholm, Sweden

27
28 12 ⁴ Department of Earth Sciences, Uppsala University, Villavägen 16 SE-752 36 Uppsala,
29
30 13 Sweden

31
32
33 14 ⁵ Department of Earth, Ocean and Atmospheric Sciences, University of British Columbia,
34
35 15 Vancouver, British Columbia, Canada

36
37 16

38
39
40 17 Corresponding author:

41
42 18 Katarzyna Walczak, Faculty of Geology, Geophysics and Environmental Protection,
43
44 19 AGH University of Science and Technology, Mickiewicza 30, 30-059 Kraków, Poland

45
46 20 Email: kwalczak@agh.edu.pl
47

48
49 21

50
51 22 Short title:

52
53 23 U-Pb zircon dating of diamondiferous gneiss, WGR
54
55
56
57
58
59
60

24 **ABSTRACT**

25 The first find of micro-diamond in the Nordøyane UHP domain of the Western Gneiss
26 Region (WGR) of the Scandinavian Caledonides reshaped tectonic models for the region.
27 Nevertheless, in spite of much progress regarding the meaning and significance of this
28 find, the history of rock that the diamonds were found in is complex and still largely
29 ambiguous. To investigate this, we report U-Pb zircon ages obtained from the exact
30 crushed sample material in which metamorphic diamond was first found. The grains
31 exhibit complicated internal zoning with distinct detrital cores overgrown by
32 metamorphic rims. The cores yielded a range of ages from the Archean to the late
33 Neoproterozoic/early Cambrian. This detrital zircon age spectrum is broadly similar to
34 detrital signatures recorded by metasedimentary rocks of the Lower and Middle
35 allochthons elsewhere within the orogen. Thus, our dating results support the previously
36 proposed affinity of the studied gneiss to the Seve-Blåhø Nappe of the Middle
37 Allochthon. Metamorphic rims yielded a well-defined peak at 447 ± 2 Ma and a broad
38 population that ranges between *c.* 437 and 423 Ma. The data reveal a prolonged
39 metamorphic history of the Fjærtøft gneiss that is far more complex than would be
40 expected for an UHP rock that has seen a single burial and exhumation cycle. The data
41 are consistent with a model involving multiple such cycles, which would provide
42 renewed support for the dunk tectonics model that has been postulated for the region.

44 Key words: geochronology, Western Gneiss Region, ultrahigh pressure metamorphism

46 **1. Introduction**

1
2
3 47 The Scandinavian Caledonides is an archetypal collisional orogen, containing some of the
4
5 48 world's best preserved and most spectacular examples of deeply buried continental rocks.
6
7 49 The mountain belt formed between the late Cambrian (Furongian) to early Ordovician
8
9 50 and the late Silurian to early Devonian (e.g. Gee *et al.* 2013 and references therein), when
10
11 51 the Iapetus basin contracted towards closure and multiple subduction-collision events
12
13 52 occurred between the hyper-extended margin of Baltica and the outboard terranes (island
14
15 53 arcs and/or microcontinents). The terminus of this period was the collision between
16
17 54 Baltica and Laurentia, with the former undergoing transient subduction deeply beneath
18
19 55 the latter (e.g. Krogh, 1977; Andersen *et al.* 1991; Brueckner & van Roermund, 2004;
20
21 56 Majka *et al.* 2014). The various subduction-collision processes produced a multitude of
22
23 57 (ultra-)high pressure (UHP-HP) rock types yielding various ages of peak metamorphism.
24
25 58 The most pronounced of the early (late Cambrian and early to mid-Ordovician) UHP-HP
26
27 59 events are those recorded in the Middle Allochthon (*sensu e.g.* Gee *et al.* 2010), which is
28
29 60 exposed along the entire length of the Scandinavian Caledonides. UHP rocks are
30
31 61 currently known from several localities spanning almost the full length of the outcrop of
32
33 62 the Middle Allochthon, a few of which contain well-established metamorphic
34
35 63 microdiamond (e.g. Smit *et al.* 2010; Janák *et al.* 2013; Majka *et al.* 2014; Gillio *et al.*
36
37 64 2015; Klonowska *et al.* 2016, 2017; Bukala *et al.* 2018). While these occurrences are
38
39 65 widely spaced and UHP metamorphism may not have been continuous or exactly
40
41 66 contemporaneous between them, subduction of the Baltica continental margin was clearly
42
43 67 an important and widespread process during the Caledonian orogenic cycle prior to the
44
45 68 final Scandian collision.
46
47
48
49
50
51
52
53
54
55
56
57
58
59
60

1
2
3 69 Vestiges of the Middle Allochthon also occur as deep infolds or tectonic intercalations
4
5 70 within the largest UHP-HP province in the Scandinavian Caledonides (Terry &
6
7 71 Robinson, 2004; Robinson *et al.* 2014), the Western Gneiss Region (WGR), which is a
8
9 72 large tectonic window in which the Baltic cratonic margin, intensively reworked,
10
11 73 emerges in the hinterland through the pile of allochthons. This giant UHP terrane
12
13 74 represents the deeply subducted margin of Baltica (Krogh, 1977; Cuthbert *et al.* 1983).
14
15 75 Here, the Middle Allochthon is intimately associated with HP or UHP Baltica basement
16
17 76 rocks (Terry & Robinson, 2004). Differences between the ages for UHP metamorphism
18
19 77 in the Middle Allochthon in Sweden (Ordovician) and in the basement orthogneisses of
20
21 78 the WGR (latest Silurian to early Devonian) suggest that inliers of the Middle Allochthon
22
23 79 in the WGR could have undergone both Ordovician and Silurian-Devonian
24
25 80 metamorphism and thus may have been subducted at least twice during the Caledonian
26
27 81 orogenic cycle.

28
29 82 The possibility of dual or even multiple subduction episodes was embodied in the ‘dunk
30
31 83 tectonics’ evolutionary model proposed by Brueckner & van Roermund (2004) and
32
33 84 Brueckner (2006) and revived by Majka *et al.* (2014), in which a continental margin is
34
35 85 repeatedly subducted into the mantle (‘dunked’) during successive collisions with arcs
36
37 86 and continental fragments during ocean closure, including the climactic final continental
38
39 87 collision. The dunk tectonics model predicts repeated UHP-HP metamorphism across
40
41 88 laterally extensive domains of the terranes now dispersed among the thrust stack in the
42
43 89 orogenic foreland. If this is the case, the early to mid-Ordovician subduction-related
44
45 90 metamorphism recorded in the Seve nappes exposed in Sweden (e.g. Janák *et al.* 2013;
46
47 91 Klonowska *et al.* 2017; Bukala *et al.* 2018) should also have affected the Blåhø Nappe
48
49
50
51
52
53
54
55
56
57
58
59
60

1
2
3 92 (Middle Allochthon) in the WGR, but would have been strongly overprinted by the late
4
5 93 Silurian-Devonian ‘Scandian’ collision between Baltica and Laurentia and the resulting
6
7 94 (U)HP metamorphism that is so spectacularly recorded in the WGR basement. Tracing
8
9
10 95 this early subduction record into the highest-grade domains of the WGR deep within the
11
12 96 orogenic core has, indeed, proved difficult thus far. (U)HP rocks in these domains mostly
13
14 97 belong to the Baltic basement and record only Siluro-Devonian (Scandian; 425-400 Ma)
15
16
17 98 overprinting. However, a well-known but enigmatic occurrence of high-grade pelitic
18
19 99 gneiss outcropping in the Nordøyane area of western Norway has yielded microdiamond
20
21
22 100 (Dobrzhinetskaya *et al.* 1995) and thus shows petrological similarity to some metapelitic
23
24 101 UHP rocks in the Seve Nappe Complex near the Caledonide foreland (Klonowska *et al.*
25
26 102 2017). To trace the history of high-grade allochthonous rocks in the WGR and ultimately
27
28 103 test the efficacy of the dunk tectonics model, we subjected zircon from this unusual
29
30
31 104 lithology to U-Pb zircon chronology. These rocks have long been ascribed to the Seve-
32
33 105 Blåhø Nappe of the Middle Allochthon (e.g. Krill, 1985) and thus may provide a record
34
35 106 of earlier metamorphic cycles that are otherwise overlooked or lacking.
36
37
38
39

40 108 **2. Geological setting**

41
42 109 This study focuses on high-grade gneisses exposed within the northern part of the WGR
43
44 110 (Fig. 1a) - a giant Baltic (U)HP terrane exposed in the high-grade core of the
45
46
47 111 Scandinavian Caledonides of western Norway (e.g. Hacker *et al.* 2010, 2015). The WGR
48
49 112 is predominantly composed of felsic-to-intermediate orthogneisses and psammitic
50
51 113 metasediments with Mesoproterozoic and Neoproterozoic protoliths derived from the
52
53
54 114 Fennoscandian craton and its pre- to syn-orogenic metasedimentary cover (the ‘para-

1
2
3 115 autochthon') rocks (e.g. Krill, 1980, 1985; Gaal & Gorbatshev, 1987; Tucker *et al.*
4
5 116 1991, 2004; Robinson *et al.* 2014; Young, 2018). Near the southeastern margin of the
6
7 117 WGR, the terrane is dominated by rocks resembling the pristine Baltican basement rocks
8
9 118 of the foreland. Towards the northwest and west, however, the basement rocks are
10
11 119 intensely *Caledonized*, i.e. reworked by Caledonian tectonism and metamorphism, and
12
13 120 show widespread evidence for (U)HP metamorphism, mainly in the form of abundant
14
15 121 pods of eclogite, but also HP or UHP felsic rocks (Krogh, 1977; Griffin & Brueckner,
16
17 122 1985; Cuthbert *et al.* 2000; Hacker *et al.* 2010). In the highest-P parts of the WGR
18
19 123 several isolated bodies of mantle-derived ultramafic rocks including dunite, garnet
20
21 124 peridotite and garnet pyroxenites appear (e.g. Brueckner *et al.* 2010), reinforcing the
22
23 125 evidence that the WGR rocks have been subducted into the mantle. The eclogite-facies
24
25 126 mineral assemblages have been pervasively overprinted by amphibolite and granulite-
26
27 127 facies parageneses associated with exhumation, decompression, partial melting and late
28
29 128 flattening and shearing (Wilks & Cuthbert, 1994; Labrousse *et al.* 2002; Hacker *et al.*
30
31 129 2010). However, the overprint was not total and fresh eclogite bodies are still frequent
32
33 130 across the WGR.

34
35
36
37
38
39 131 An exceptional effort in multi-method chronology during the past decades has
40
41 132 constrained the age of (U)HP metamorphism to between 425 and 400 Ma, i.e. during the
42
43 133 Scandian Orogeny (Hacker *et al.* 2010, and references therein). During this time, the
44
45 134 hyper-extended Baltic margin was buried beneath the Laurentian continental lithosphere
46
47 135 at rates of *c.* 5 mm yr⁻¹ (Cutts & Smit, 2018), ultimately reaching depths of 100 km or
48
49 136 more (Hacker *et al.* 2010 and references therein). The (U)HP stage was followed by
50
51 137 amphibolite-facies overprinting between 400-385 Ma (Terry *et al.* 2000; Kylander-Clark
52
53
54
55
56
57
58
59
60

1
2
3 138 *et al.* 2008; Krogh *et al.* 2011) and cooling below 400°C by *c.* 375 Ma (Hacker & Gans,
4
5 139 2005; Root *et al.* 2005; Walsh *et al.* 2013).

6
7
8 140 The WGR basement is bounded by the major Caledonide thrust complexes of the Middle
9
10 141 and Upper Allochthons. The Middle Allochthon comprises discrete lithotectonic units
11
12 142 that vary along the orogen. In southern Norway it is dominated by Proterozoic crystalline
13
14 143 complexes with metasandstones, e.g. the Jotun Nappe Complex, Lindås and Jaeren
15
16 144 Nappes. In central and northern Sweden and northern Norway Caledonian high-grade
17
18 145 rocks, e.g., migmatite, granulite, metasandstone, augen gneiss, amphibolite and eclogite
19
20 146 of the Seve and Kalak Nappe Complexes dominate (see e.g. Gee *et al.* 2013 and
21
22 147 references therein). The Middle Allochthon is interpreted to represent the distal
23
24 148 continental margin of Baltica and may include micro-continental fragments (Cuthbert *et*
25
26 149 *al.* 1983; Emmett, 1996; Andersen *et al.* 1991; Gee *et al.* 2010, 2013). The Upper
27
28 150 Allochthon contains a diverse assemblage of ophiolite and arc rocks that originated
29
30 151 outboard of Baltica within the Iapetus Ocean between 490-440 Ma (Stephens & Gee,
31
32 152 1985, 1989; Stephens, 1988).

33
34
35 153 Both allochthons underwent reworking and final emplacement onto the Baltican
36
37 154 continental margin during the Scandian collision. In addition, however, they show
38
39 155 evidence of earlier tectonometamorphic episodes. In the large Seve Nappe Complex in
40
41 156 Sweden, as well as in small slivers of allochthonous rocks in southwesternmost Norway,
42
43 157 this is indicated by (U)HP metamorphism at *c.* 460 – 445 Ma, which has been attributed
44
45 158 to a pre-Scandian arc-continent collision (e.g. Brueckner *et al.* 2004; Brueckner & Van
46
47 159 Roermund, 2004, 2007; Smit *et al.* 2010; 2011; Majka *et al.* 2012, 2014; Root & Corfu,
48
49 160 2012; Grimmer *et al.* 2015; Klonowska *et al.* 2016, 2017; Fassmer *et al.* 2017). Yet older,
50
51
52
53
54
55
56
57
58
59
60

1
2
3 161 c. 500-485 Ma, (U)HP metamorphic rocks are also recognized in the Seve Nappe
4
5 162 Complex of northern Sweden (Mørk *et al.* 1988, Root & Corfu, 2012, Barnes *et al.*
6
7 163 2019).

8
9
10 164 In the foreland regions of southern Norway, and central and northern Sweden an
11
12 165 additional nappe complex, the Lower Allochthon, underlies the Middle Allochthon and
13
14 166 comprises thrust repetitions of basement and sedimentary cover derived from the
15
16 167 Fennoscandian shield (hereafter termed the Baltican basement). These rocks record the
17
18 168 long-lived thrusting of the allochthons onto the Baltic margin during the Scandian.

19
20 169 Outcropping within the high-grade sections of the Baltican basement in the WGR are
21
22 170 belts (inliers) of more diverse lithological assemblages including psammitic and pelitic
23
24 171 metasediments, anorthosites and distinctive megacrystic augen gneisses. Such
25
26 172 assemblages may represent basement-cover repetitions derived from the Baltica slab (i.e.
27
28 173 Lower Allochthon), although they commonly also exhibit lithological similarities with
29
30 174 the Middle Allochthon in the main allochthon exposures (Krill, 1980; Robinson, 1995;
31
32 175 Robinson *et al.* 2014).

33
34 176 These inliers of the allochthons are conventionally regarded as being above the main
35
36 177 mass of orthogneisses in the tectonostratigraphy and down-folded into these (Krill, 1985;
37
38 178 Tucker *et al.* 2004; Robinson & Hollocher, 2008). The complete sequence is (from base
39
40 179 to top above the Baltican basement) the Risberget nappe (augen orthogneisses,
41
42 180 anorthosites, metagabbros); Saetra Nappe (quartzite with deformed dykes of
43
44 181 metadolerite); Blåhø Nappe (high grade metapelite, calc-silicate, marble, amphibolite and
45
46 182 mafic granulite); Støren Nappe (ophiolitic and arc rocks of greenschist to low
47
48 183 amphibolite facies). The last of these is part of the Upper Allochthon, while the others are

49
50
51
52
53
54
55
56
57
58
59
60

1
2
3 184 correlated with the Middle Allochthon. The Blåhø Nappe is correlated with the high-
4
5 185 grade Middle Seve Nappe in the main allochthon outcrop in central and northern Sweden.
6
7 186 Their structural evolution has been established in the north-eastern WGR in the
8
9 187 Trollheimen-Trondheim district (Robinson *et al.* 2014), where tectonostratigraphic units
10
11 188 of the Middle Allochthon were thrust over the Baltican basement, then this combined
12
13 189 sequence was folded to form a basement cored nappe that was translated eastwards
14
15 190 towards the foreland along the late, out-of-sequence, Storli Thrust. The nappe core
16
17 191 contains eclogite dated at 425 ± 10 Ma (Beckman *et al.* 2013), but the lower basement
18
19 192 unit below the thrust is devoid of eclogite. The same sequence can be traced to
20
21 193 Moldefjord and the southern part of the Nordøyane, far to the west (Fig. 1; see also
22
23 194 Robinson, 1985). A similar structural evolution was demonstrated by Young (2018) in
24
25 195 the central WGR, where allochthonous rocks ('mixed rocks') were tectonically
26
27 196 imbricated and infolded following emplacement onto the Baltica basement along major
28
29 197 foreland-vergent shear zones.
30
31 198 The allochthons have also been mapped out eastwards into the main allochthon outcrop
32
33 199 in the frontal zone in central Sweden (e.g. Gee *et al.* 2010). Here, the Middle Allochthon
34
35 200 is more continuously exposed, is several km thick and bounded by major thrusts. In the
36
37 201 WGR, however, these nappes are either extremely attenuated to a few meters in thickness
38
39 202 or excised entirely (Robinson, 1995). In the Trondheim area and southwestwards to
40
41 203 Moldefjord the upper boundary of the Middle Allochthon against the Upper Allochthon is
42
43 204 a major west-vergent, late orogenic ductile detachment fault, the Agdenes Detachment
44
45 205 (Robinson *et al.* 2014).
46
47 206
48
49
50
51
52
53
54
55
56
57
58
59
60

207 **2a. Nordøyane ultra-high pressure domain**

208 The sample investigated here comes from the island of Fjørtoft (Fig. 1b) in the
209 Nordøyane archipelago, immediately west of Moldefjord, which lies within the
210 northernmost UHP domain of the WGR (Root *et al.* 2005). The Middle Allochthon
211 sequence established in the Trollheimen-Moldefjord area has been mapped across the
212 Nordøyane by Terry & Robinson (2003, 2004). The lithology of interest is a pelitic
213 garnet-kyanite gneiss in an assemblage also including biotite-garnet migmatite, calc-
214 silicate, marble and eclogite, all correlated with the Blåhø Nappe. The structural and
215 fabric evolution in the Nordøyane provides key constraints in the interpretation of the
216 zircon dating set out in the following sections.

217 There are two major structural domains in Nordøyane (Terry & Robinson, 2013, 2014)
218 separated by a major late-orogenic, steep sinistral discontinuity, the Åkre-Midøy shear
219 zone. To its south the structural evolution resembles the situation in Trollheimen and
220 Moldefjord. The northern structural domain has been brought in against the southern
221 domain from the NE by motion along the Åkre-Midøy shear zone (Terry & Robinson,
222 2003, 2004). Evidence for UHP metamorphism is found in the Baltican basement, the
223 allochthons and in mantle-derived ultramafic massifs (Dobrzhinetskaya *et al.* 1995; Terry
224 *et al.* 2000; Carswell *et al.* 2006; Vrijmoed *et al.* 2006; Spengler *et al.* 2009; Butler *et al.*
225 2013). The Middle Allochthon is only represented by the Blåhø Nappe, which has been
226 folded into the core of a large recumbent, isoclinal synform with dioritic to granitoid
227 gneisses of the Baltican basement on either limb (Terry & Robinson, 2004). The contact
228 is coincident with an eclogite- (or high-P granulite-) facies shear zone that extends
229 through Blåhø and a few hundred meters into the adjacent basement, and in which

1
2
3 230 mylonite lineations and rotated porphyroclasts show top-SE shear sense when the folds
4
5 231 are restored to pre-folding geometry (Terry *et al.* 2000a; Terry & Robinson, 2004). These
6
7 232 fabrics are associated with transformation of two metagabbro lenses to eclogite (Mørk,
8
9 233 1985; Terry & Robinson, 2004) dated at 410 ± 2 Ma (Krogh *et al.* 2011; see also Mørk &
10
11 234 Mearns, 1986). Terry *et al.* (2000a) and Terry & Robinson (2004) proposed that this
12
13 235 shear zone emplaced the UHP Blåhø Nappe over Baltican basement that had only
14
15 236 experienced HP eclogite conditions, but Carswell *et al.* (2006) showed that nearby
16
17 237 eclogites in the Baltican basement equilibrated under UHP conditions, in which case the
18
19 238 shear zone operated during exhumation and the metamorphic assemblages are retrograde.
20
21 239 It remains possible, however, that all the UHP eclogites are part of the sheared basement
22
23 240 pediment attached to the underside Blåhø Nappe and a cryptic HP basement unit lies at a
24
25 241 deeper structural level.
26
27 242 Lenses of garnet peridotite and pyroxenite derived from subcontinental mantle decorate
28
29 243 the basement-cover contact and are scattered through the Baltica basement in a zone a
30
31 244 few hundred meters below it, confirming the existence of a fundamentally important
32
33 245 tectonic contact here. Late fabrics defined by UHP mineral assemblages in these garnet
34
35 246 pyroxenites at Bardane, Fjørtoft and Flemsøy give $P \approx 6$ GPa at sub-geotherm
36
37 247 temperatures for cratonic mantle (e.g. Vrijmoed, van Roermund & Davies, 2006;
38
39 248 Scambelluri, van Roermund & Pettke, 2010). A mineral isochron age of 429 ± 3.1 Ma for
40
41 249 this mineral assemblage was interpreted to represent an early stage in the subduction of
42
43 250 the outermost Baltica continental margin (Spengler *et al.* 2009).
44
45 251 Two kyanite eclogites from the Blåhø Nappe very close to its lower boundary record P-T
46
47 252 conditions overlapping the diamond stability field (Terry *et al.* 2000) and one of these
48
49
50
51
52
53
54
55
56
57
58
59
60

1
2
3 253 gives a Lu-Hf mineral age of 404.9 ± 7.9 Ma (Cutts & Smit, 2018). A distinctive feature
4
5 254 of the Blåhø in the Nordøyane and Moldefjord area is that eclogites and other mafic rocks
6
7
8 255 are a common part of the rock assemblage, while these are less common in the main
9
10 256 outcrop of the equivalent Seve Nappe in Sweden. An eclogite from the island of Gossa,
11
12 257 adjacent to Fjørtoft, gives a Scandian Sm-Nd mineral isochron age of 413.9 ± 3.7 Ma
13
14 258 (Kylander-Clarke, 2009). Another two from the mainland along strike from Nordøyane
15
16
17 259 have given Scandian ages for (U)HP metamorphism (418 ± 27 Ma, Tverfjell north of
18
19 260 Molde; Griffin & Brueckner, 1985 and 415.2 ± 0.6 Ma, Averøya, near Kristiansund;
20
21 261 Krogh *et al.* 2011).

22
23
24 262 The age of UHP metamorphism in the Baltican basement in the northern domain is
25
26 263 constrained by a U-Pb zircon date of 405 ± 1 Ma from an eclogite at Midsund, Otrøy
27
28 264 (Krogh *et al.* 2011) although, puzzlingly, Kylander-Clark *et al.* (2007) derived Lu-Hf
29
30 265 garnet and Sm-Nd garnet – whole-rock ages for this eclogite of 380 ± 14 Ma and 388
31
32 266 ± 10 Ma, respectively, which are significantly younger than any other UHP eclogite ages
33
34 267 in the WGR; they are, however, Scandian. Zircons from the Svartberget microdiamond-
35
36 268 bearing metasomatic veins in garnet websterite within Baltican basement orthogneiss
37
38 269 give a robust U-Pb (LA-ICP-MS) age for a cluster of concordant points of 410.6 ± 2.6
39
40 270 Ma (Quas-Cohen, 2013) which is taken to date metasomatism and microdiamond
41
42 271 formation. Samples from the same body also yielded significantly younger and perhaps
43
44 272 less robust dates by U-Pb on zircon using ID-TIMS, which gave a discordia intercept of
45
46 273 397.2 ± 1.2 Ma (Vrijmoed *et al.* 2013) and Sm-Nd mineral isochrons yielded dates of 393
47
48 274 ± 3 Ma to 381 ± 6 Ma (Vrijmoed *et al.* 2008) interpreted to be cooling ages.
49
50
51
52
53
54
55
56
57
58
59
60

1
2
3 275 Overall, it is possible to reconstruct an evolution for this northern, UHP domain, based on
4
5 276 the tectonic model of Terry & Robinson (2004) in Nordøyane and adjacent areas:

7
8 277 1) The Blåhø Nappe is emplaced on to the Baltica basement (time uncertain but
9
10 278 before 430 Ma).

12 279 2) Baltica basement and Blåhø Nappe are subducted deep enough to capture mantle
13
14 280 ultramafic rocks (at least 200 km) at ~430 Ma during the early stages of the Scandian
15
16
17 281 continent-continent collision.

19 282 3) UHP eclogites form, or continue to equilibrate, in both units until ~410 Ma.

21 283 4) The Blåhø Nappe and a detached pediment of Baltica Basement rise as a nappe
22
23 284 over the (still descending?) deeper basement, generating the top-southeast HP
24
25 285 eclogite or HP granulite shear fabrics (≤ 410 Ma).

28 286 The available evidence favours a common, roughly synchronous, Scandian diamond-
29
30 287 eclogite facies metamorphism for both the Blåhø Nappe and the Baltica basement in the
31
32 288 northern domain of Nordøyane, with a basement-cover nappe similar in geometry to the
33
34 289 Trollheimen-Moldefjord region but operating at much deeper levels. The whole
35
36 290 basement-cover package in both northern and southern structural domains has then been
37
38 291 refolded about upright, folds associated with a pervasive, sinistral or top-west
39
40 292 amphibolite-facies fabric with horizontal lineations and fold axes (Terry & Robinson,
41
42 293 2003) dated at 396 Ma from boudin-neck pegmatites (Krogh *et al.* 2011). (U)HP
43
44 294 lithologies and fabrics are preserved only as rare relics where they have survived
45
46 295 overprinting by the late-orogenic deformation. Any signature of pre-Scandian
47
48 296 metamorphism must have survived both this and the Scandian UHP tectono-
49
50 297 metamorphism.
51
52
53
54
55
56
57
58
59
60

1
2
3 298
45 299 **3. Sample Description**
6

7
8 300 The sample investigated here was collected from an old quarry at Vågholmane, just north
9
10 301 of the ferry terminal. It is the residue of the same sample (ID: Fj-19; Fig. 2) from which
11
12 302 Dobrzhinetskaya *et al.* (1995) extracted metamorphic diamond by a chemical dissolution
13
14 303 process performed on a crushed block. The lithology has been described previously by
15
16 304 Dobrzhinetskaya *et al.* (1995), Holder *et al.* (2015), Liu & Massonne (2019) and Terry *et*
17
18 305 *al.* (2000b); the latter's sample (recoded by them as UHP1) was a thin section cut from
19
20 306 the microdiamond-bearing sample, so is the same sample block from which our zircons
21
22 307 were sourced. It is composed of garnet, kyanite, phlogopite, K-feldspar, plagioclase,
23
24 308 quartz, graphite and additionally rutile, sulphides, monazite and zircon. Garnet is
25
26 309 abundant, pale mauve-coloured, typically 0.5-1.0 cm in size, and locally occurs as
27
28 310 globular megacrysts of 3-5 cm surrounded by conspicuous coronas of felsic minerals. It
29
30 311 shows distinctive zoning with low Ca garnet cores (Terry *et al.* 2000b; Holder *et al.*
31
32 312 2015; Liu & Massone, 2019; authors' unpublished data) enclosing abundant, small
33
34 313 needles of kyanite. High Ca rims contain larger inclusions of kyanite, quartz, rutile,
35
36 314 graphite, perthitic feldspar and sulphides, along with rationally orientated needles of
37
38 315 rutile. It has not often been recognised that the rock is a blastomylonite with streaky
39
40 316 appearance suggesting pre-tectonic migmatization. Relics of granitic (partial) melt are
41
42 317 preserved as embayments and inclusions in the garnet rims and are composed of perthite,
43
44 318 quartz and phlogopite. Monazite and zircon are found in both cores and rims of garnet.
45
46 319 The rock matrix is generally composed of fine-grained plagioclase and K-feldspar (from
47
48 320 the breakdown of coarse perthite and garnet), quartz and large flakes of phlogopite and
49
50
51
52
53
54
55
56
57
58
59
60

1
2
3 321 graphite. No microdiamond has yet been found in-situ, nor any other (U)HP phases,
4
5 322 although muscovite inclusions in garnet associated with phlogopite may be relics after
6
7 323 phengite. Larsen *et al.* (1998), who described the rock as a 'felsic granulite', estimated P
8
9
10 324 = 16-23 kbar at 600-800 °C for the matrix assemblage assuming equilibrium with garnet
11
12 325 rims. However, the recent detailed study by Liu & Massonne (2019) suggests that this
13
14 326 rock underwent most probably a prolonged anticlockwise P-T path, with peak conditions
15
16
17 327 around 1.35-1.45 GPa and 770-820 °C and an earlier equilibration event at *c.* 1.35-1.45
18
19 328 GPa and 770-820 °C.

20
21 329 In the field, two linear fabrics can be recognised in the Blåhø Nappe felsic gneisses
22
23 330 (Terry *et al.* 2000; Terry & Robinson, 2004). The earlier fabric is represented by the
24
25 331 sample UHP1 described above, and is defined by mineral-aggregate rods and common
26
27 332 orientation of kyanite. Kinematic indicators on steep foliation surfaces including rotated
28
29 333 kyanite and garnet porphyroclasts indicating north-side-up shear that translates to top-
30
31 334 southeast shear when the effects of later folding are removed, as found in the eclogite-
32
33 335 facies shear zones described above. Terry & Robinson (2004) attributed the tectonite
34
35 336 fabrics of the basement metagabbros and dioritic orthogneisses to the same kinematic
36
37 337 system as this early fabric in the Blåhø Nappe gneiss, suggesting that it operated at about
38
39 338 410 Ma, postdating an episode of partial melting, and was related to foreland directed
40
41 339 transport of a (U)HP basement with associated Seve-Blåhø allochthon.

42
43 340 The later fabric is a mineral-aggregate rodding lineation defined by sillimanite replacing
44
45 341 deformed, fish-shaped kyanite porphyroclasts or disseminated in the matrix, which
46
47 342 displays extreme grain-size reduction. Garnet porphyroclasts are dismembered and strung
48
49 343 out in the lineation (Terry *et al.* 2000b). Mica- and sillimanite-rich elements of the matrix
50
51
52
53
54
55
56
57
58
59
60

1
2
3 344 display S-C fabrics. The lineations and associated fold axes are roughly horizontal and
4
5 345 the kinematic indicators show consistent top-west or sinistral shear. This fabric overprints
6
7 346 and re-orientates the steeper kyanite lineation. This late top-west shear fabric also
8
9
10 347 dominates large parts of the allochthons and some of the adjacent basement gneisses in
11
12 348 the westernmost WGR, indicating a top-to-the-west transport. This was related to reversal
13
14 349 of motion on the major thrust surfaces, the development of Agdenes Detachment and
15
16 350 Nordfjord-Sogn Detachment Zone and the late-orogenic Old Red Sandstone basins
17
18 351 (Norton, 1987; Wilks & Cuthbert, 1994; Brueckner & Cuthbert, 2013; Robinson *et al.*
19
20 352 2014; Young, 2018).

21
22
23 353 Zircons in the mineral separate that we obtained from sample Fj-19 contains micro-
24
25 354 inclusions of quartz, feldspar, mica, apatite, graphite and rutile (H.-J. Massonne, pers.
26
27 355 comm. 2005). No HP or UHP indicator micro-inclusions such as diamond, coesite,
28
29 356 phengitic mica or jadeitic clinopyroxene have been found. Monazite from the
30
31 357 microdiamond-yielding sample has been analysed by electron microprobe (Th-U-total
32
33 358 Pb) and secondary ionization mass spectrometry (U-Th-Pb), along with a sample of
34
35 359 porphyroclastic mylonite with the younger lineation from 1km west of Vågholmane
36
37 360 (Terry *et al.* 2000; their samples UHP1 and 929, respectively). The analyses yield a
38
39 361 cluster of dates between 1100 and 950 Ma, a few scattered dates between 900 Ma and
40
41 362 500 Ma, and other clusters at *c.* 415, 408, 395 Ma and *c.* 375 Ma. The older dates of
42
43 363 415.0 ± 6.8 Ma (SIMS) and 408.0 ± 5.6 Ma (EPMA) were obtained from the same
44
45 364 monazite inclusions in garnet and have been interpreted as indicating the maximum age
46
47 365 of garnet growth. The two youngest dates were interpreted to represent different phases
48
49 366 of exhumation from deep subduction conditions. Recently, Holder *et al.* (2015) have also
50
51
52
53
54
55
56
57
58
59
60

1
2
3 367 performed *in-situ* monazite U-Th-Pb dating using laser ablation split stream inductively
4
5 368 coupled plasma mass spectrometry. These authors dated two samples of the same rock
6
7
8 369 and obtained the following results: a cluster of ages between 1200 and 900 Ma,
9
10 370 Caledonian concordia ages peaking at 431.1 ± 1.7 Ma, 426.8 ± 1.7 Ma, 425.5 ± 3.0 , 393
11
12 371 ± 3.0 Ma and 391.3 ± 2.7 Ma. Contrasting REE patterns for inclusions and matrix grains
13
14 372 dated at *c.* 425 Ma suggest that garnet growth took place at this time, but other inclusions
15
16 373 as young as *c.* 390 Ma may indicate either continued growth to this time or re-setting. A
17
18 374 continued growth of monazite is also suggested by Liu & Massonne (2019), who reported
19
20 375 Th-U-total Pb monazite dates spanning from 460 to 380 Ma and interpreted them to
21
22 376 reflect a prolonged residence time under relatively high temperatures due to two burial
23
24 377 events that have never reached UHP conditions. We differ by not ruling out diamond-
25
26 378 stable P-T conditions at some time during its history, as some stages of the rock history
27
28 379 may have been destroyed during overprinting, for example during partial melting.
29
30
31 380 To our knowledge, no zircon dates have so far been documented in the literature for this
32
33 381 unusual and widely studied rock.
34
35
36
37
38
39

40 383 **4. Methods**

41
42 384 Uranium-lead dating was performed on zircon grains initially separated by D. A.
43
44 385 Carswell and H.-J. Massonne for studies of inclusions; the separate was kindly provided
45
46 386 by H.-J. Massonne, who mounted and polished the grains in an epoxy mount. The zircon
47
48 387 grains are from the same rock volume from which micro-diamond was isolated
49
50 388 (Dobrzhinetskaya *et al.* 1995). The grains are 100-250 μm in length and were polished to
51
52 389 their geometric core. U-Pb dating of zircon was performed at the Swedish Museum of
53
54
55
56
57
58
59
60

1
2
3 390 Natural History, Stockholm, using a Nu Instruments Plasma II multi-collector inductively
4
5 391 coupled plasma mass spectrometry (MC-ICPMS) instrument coupled to an ESI
6
7 392 NWR193UC excimer laser ablation system. The m/z (mass-to-charge ratio)
8
9 393 corresponding to masses 202, 204, 206, 207 and 208 were measured on ion counters, and
10
11 394 those corresponding to 232, 235, and 238 were measured on Faraday collectors. The laser
12
13 395 was fired for 35 s with a fluence of 3.5 J/cm^2 , a pulse rate of 8 Hz and a spots size of 15
14
15 396 μm . Helium was used as a sample carrier gas (0.3 l/min) to flush the laser cell and was
16
17 397 mixed with argon sample gas (0.9 l/min) before entering the ICP-MS. Analyses were
18
19 398 corrected for mass bias and elemental fractionation using the protocols of Kooijman *et al.*
20
21 399 (2012). The 91500 zircon reference material (1065 Ma; Wiedenbeck *et al.* 1995) was
22
23 400 used for normalization and repeated analyses indicated external reproducibility of 1.0%
24
25 401 2RSD for the ^{207}Pb - ^{206}Pb age and 1.2% 2RSD for the ^{206}Pb - ^{238}U age ($n = 58$). Accuracy
26
27 402 was assessed by analysing the secondary reference zircons Plešovice (337 Ma; Sláma *et*
28
29 403 *al.* 2008), GJ-1 (609 Ma; Jackson *et al.* 2004) and Temora 2 (417 Ma; Black *et al.* 2004).
30
31 404 We obtained $336 \pm 11 \text{ Ma}$ (Plešovice; $n = 8$), $606 \pm 3 \text{ Ma}$ (GJ-1; $n = 8$), and $416 \pm 9 \text{ Ma}$
32
33 405 (Temora 2; $n = 5$), all of which agree within 1% of published age estimates for these
34
35 406 materials. Data reduction employed in-house Excel macros. Age calculations and
36
37 407 construction of concordia diagrams were prepared using the Excel extension Isoplot 3.75
38
39 408 (Ludwig, 2012). All uncertainties are reported at the 2σ level. Age data are illustrated in
40
41 409 Figure 4 and presented in Table 1.
42
43
44
45
46
47
48
49
50

51 411 **5. Results**

52
53
54
55
56
57
58
59
60

1
2
3 412 Separated zircon grains are spherical or slightly elongated in shape, with rounded edges.
4
5 413 Cathodoluminescence (CL) images reveal complex internal structure and most zircons
6
7 414 display obvious multi-stage growth features (Fig. 3). Most commonly, zircon grains
8
9 415 display cores with well-defined concentric oscillatory zoning, typical of magmatic zircon,
10
11 416 which is overgrown by a bright-CL rims. Such rims show no visible zoning and are likely
12
13 417 of metamorphic origin. U-Pb isotope data obtained from the dated grains are presented in
14
15 418 Table 1 and reveal a complex multi-component age signature. The majority of dates older
16
17 419 than 700 Ma were obtained from zircon cores and display significant degrees of
18
19 420 discordance (Figs. 4a, d, f). Several ^{207}Pb - ^{206}Pb date clusters can be distinguished among
20
21 421 the obtained results: (1) a Neoproterozoic cluster between 2.8-2.5 Ga ($n = 6$); (2) a small
22
23 422 cluster in the Mesoproterozoic (1.5-1.3 Ga; $n = 3$); (3) late Mesoproterozoic to early
24
25 423 Neoproterozoic dates between 1.1-0.9 Ga ($n = 6$); and (4) a group of Neoproterozoic
26
27 424 dates between 0.9-0.7 Ga ($n = 7$). A small group of three concordant dates between 540-
28
29 425 520 Ma (Table 1) was also obtained, one of which is from a core domain, whereas the
30
31 426 other two were obtained from rims. A notable number of Caledonian spot dates range
32
33 427 from 450 to 400 Ma (Fig. 4b). Two subgroups of dates can be distinguished among the
34
35 428 concordant results (Fig. 4e). Five of the oldest Caledonian dates cluster between 450-440
36
37 429 Ma and give a concordia age of 446.6 ± 2.1 Ma (Fig. 4c). Another cluster of concordant
38
39 430 dates is observed between 437-423 Ma, and yield a weighted average ^{206}Pb - ^{238}U date of
40
41 431 428.3 ± 1.7 Ma. The three youngest dates are *c.* 415 Ma and younger.
42
43
44
45
46
47
48
49
50

51 433 **6. Discussion**

52 434 **6.a. Provenance and exotic nature of the Fjortoft diamondiferous gneiss**

53
54
55
56
57
58
59
60

1
2
3 435 The oldest detrital ages (2.8-2.5 Ga) are not known from the Baltica basement rocks of
4
5 436 the WGR. Such detrital ages are, however, observed in the Lower and Middle
6
7 437 Allochthons in Sweden (e.g. Gee *et al.* 2014, 2015; Ladenberger *et al.* 2014), as well as
8
9 438 in southwesternmost Norway (Smit *et al.* 2011). Two younger groups, 1.5-1.3 Ga and
10
11 439 1.1-0.9 Ga, correspond to the Gothian and Sveconorwegian orogenies, respectively. The
12
13 440 older group is widespread in the WGR and marks a major episode of magmatism within
14
15 441 the Fennoscandian basement (e.g. Corfu & Andersen, 2002; Tucker *et al.* 2004; Krogh *et*
16
17 442 *al.* 2011). The younger group is also common across the WGR, both in the allochthons
18
19 443 and in the basement; it derives from magmatism and metamorphism during the
20
21 444 Sveconorwegian Orogeny (e.g. Tucker *et al.* 1990; Bingen & van Breemmen, 1998;
22
23 445 Bingen *et al.* 2001; Røhr *et al.* 2004; Walsh *et al.* 2007; Des Ormeau *et al.* 2015; Corfu &
24
25 446 Andersen, 2002). Terry *et al.* (2000) recognised a similar group of ages among monazite
26
27 447 cores from the diamond-bearing gneiss on Fjørtoft. These age components clearly
28
29 448 establish the Baltic provenance of this rock, indicating that its sedimentary protolith was
30
31 449 deposited within the Baltic continental realm or its Iapetus Ocean margin.

32
33 450 Neoproterozoic ages between 0.9 and 0.7 Ga are less common within the Baltic basement
34
35 451 (Bingen & Solli, 2009). They are, however, reported from detrital zircons in the Seve
36
37 452 Nappe Complex in Sweden (Gee *et al.* 2014) and igneous bodies of similar age are also
38
39 453 known from other parts of the Middle Allochthon. Paulsson & Andréasson (2002)
40
41 454 reported *c.* 845 Ma U–Pb age of the Vistas granite in the Seve Nappe Complex in
42
43 455 northern Sweden, while *c.* 840 and 710 Ma ages are typical of granitic magmatism in the
44
45 456 Sørøy-Seiland and Havvatnet nappes of the Kalak Nappe Complex in northernmost
46
47 457 Norway (Kirkland *et al.* 2006). Walker *et al.* (2016) have also reported a *c.* 725-700 Ma
48
49
50
51
52
53
54
55
56
57
58
59
60

1
2
3 458 tectonothermal event recorded in the Caledonides of Shetland. Several of these possible
4
5 459 sources derive from Neoproterozoic magmatism and tectonism (Renlandian and
6
7 460 Knoydartian) whose products subsequently involved in the northern Iapetus-Caledonide
8
9 461 cycle (Cawood *et al.* 2010). The exact source of zircons with 0.9-0.7 Ga ages in the
10
11 462 Fjørtoft sample remains unresolved, but it is clear that these data represent an exotic
12
13 463 component acquired when the sedimentary protolith was located in a palaeogeographic
14
15 464 location distal to the Baltic craton.
16
17

18
19 465 A similar explanation may be proposed for the small group of 540 to 520 Ma ages, which
20
21 466 were also obtained by Terry *et al.* (2000), but left them uninterpreted. The dates are
22
23 467 concordant and form a distinct cluster, indicating that they have geological meaning.
24
25 468 Components of similar age are extremely rare in the present-day Scandinavian
26
27 469 Caledonides, and are mainly restricted to the Kalak Nappe Complex (e.g. Roberts *et al.*
28
29 470 2010). Interestingly, dates in the range 650-500 Ma are rare but persistently found in the
30
31 471 mantle-derived ultramafic rocks and enclosed eclogite in Nordøyane (Jamtveit *et al.*
32
33 472 1991; Spengler *et al.* 2009) and in the central WGR (Medaris *et al.* 2018), suggesting
34
35 473 magmatism or tectonism in the Iapetus realm during this interval that may have also had
36
37 474 a crustal expression.
38
39
40
41

42 475 The spectrum of different age populations further distinguishes the Fjørtoft gneiss from
43
44 476 the adjacent basement orthogneisses and confirms its profoundly allochthonous nature
45
46 477 and reinforces its correlation with the Seve-Blåhø Nappe. Moreover, it suggests a
47
48 478 previously unrecognised link between this lithotectonic unit and the terranes of the north-
49
50 479 Norwegian and Swedish Caledonides.
51
52
53

54 480
55
56
57
58
59
60

481 **6.b. Caledonian ages and evidence for double-dunking**

482 U-Pb zircon dates from the Fjørtoft gneiss corresponding to the span of the Caledonian
483 orogenic cycle cluster around *c.* 447 Ma and *c.* 437-423 Ma with three younger dates $\leq c.$
484 415 Ma. The oldest age of these mentioned above was not identified in published
485 monazite age studies by Terry *et al.* (2000b) or Holder *et al.* (2015). This age is
486 significantly earlier than almost all previous higher-precision ages for (U)HP-HT
487 metamorphism in the WGR.

488 This Ordovician age peak may be compared with **dates in** other outcrops of the
489 allochthons in the WGR. Zircon U-Pb dates of 470-430 Ma were reported for eclogites in
490 allochthonous units (Blåhø Nappe?) in the western and eastern-central parts of the WGR
491 but were attributed to protolith ages (Walsh *et al.* 2007 - **discordant dates**; DesOrmeau *et*
492 *al.* 2015). We speculate that these are lower Palaeozoic metavolcanics similar to the
493 layered eclogites described in the Blåhø Nappe on Fjørtoft by Terry & Robinson (2004)
494 and on the mainland north of Molde by Carswell & Harvey (1985). Walsh *et al.* (2007)
495 also reported a protolith (detrital?) zircon age of 480 ± 12 Ma from a pelite in the Blåhø
496 Nappe. However, our zircon ages are clearly metamorphic and do not represent growth in
497 magmatic protoliths. In contrast, Gordon *et al.* (2016) presented U-Pb zircon age
498 populations of *c.* 467 and *c.* 439 Ma obtained from leucosomes in metapelites of the
499 Seve-Blåhø Nappe north of Trondheim, which they interpreted to represent (U)HP zircon
500 growth and subsequent migmatization.

501 The younger of our two larger Caledonian U-Pb zircon age-peaks matches well with the
502 timing of Ca-rich garnet rims as indicated by *in-situ* monazite ages of *c.* 425 Ma and
503 perhaps as old as 430 Ma, (Holder *et al.* 2015) corresponding to an episode of

1
2
3 504 migmatism evidenced by granitic melt inclusions enclosed in Ca-rich garnet rims. It is
4
5 505 also not much younger than the earliest ages attributed to Scandian subduction of the
6
7 506 Baltica margin around 430 Ma as indicated by garnet pyroxenites in mantle-derived
8
9
10 507 ultramafites in Nordøyane (Jamtveit *et al.* 1991; Spengler *et al.* 2009) and elsewhere
11
12 508 (Medaris *et al.* 2018). These ages are all significantly older than the timing of HP-
13
14 509 eclogite facies SE-vergent shearing involving the metagabbros in Nordøyane (Terry *et al.*
15
16 510 2000a; Terry & Robinson, 2004) at 410 ± 2 Ma (Krogh *et al.* 2011) which has been
17
18 511 correlated with the SE-vergent shear overprinting the migmatite fabric in the Fjortoft
19
20 512 gneiss. This puts a younger age bracket on the duration of migmatism. Also, ages
21
22 513 around 410 Ma are relatively scarce in our dataset, suggesting that during this foreland-
23
24 514 directed shearing little new zircon was generated, and/or there was little resetting of the
25
26 515 zircon U-Pb isotopic system.

27
28
29
30 516 The late Ordovician age components in our dataset (*c.* 447 Ma) are uncommon or absent
31
32 517 in the WGR, but widely recognised within the Seve Nappe Complex of Jämtland in
33
34 518 Sweden and in tectonic slivers of probable Middle Allochthon rocks in southwesternmost
35
36 519 Norway (e.g. Brueckner *et al.* 2004; Brueckner & van Roermund, 2007; Smit *et al.* 2011;
37
38 520 Majka *et al.* 2012; Root & Corfu, 2012; Ladenberger *et al.* 2014; Grimmer *et al.* 2015;
39
40 521 Klonowska *et al.* 2017; Fassmer *et al.* 2017). These terranes record a mid- to late
41
42 522 Ordovician episode of (U)HP metamorphism. The lithologies in the Åreskutan Nappe,
43
44 523 Middle Seve Nappe in Jamtland, central Sweden are similar to the Fjortoft gneiss in that
45
46 524 they are metapelitic sillimanite or kyanite-bearing migmatites that record a pre-
47
48 525 migmatite, diamond-stable UHP metamorphism. Granulite-facies metamorphism and
49
50 526 migmatism has been dated at *c.* 439 Ma during decompression and partial melting,
51
52
53
54
55
56
57
58
59
60

1
2
3 527 following UHP metamorphism at *c.* 455 Ma (Majka *et al.* 2012). Emplacement of these
4
5 528 rocks as a hot nappe above the Lower Seve Nappe Complex was dated from monazite in
6
7 529 basal mylonites at 424 ± 6 Ma (Majka *et al.* 2012) which was within error of the age for
8
9 530 crystallisation of post-migmatite, pre-mylonite pegmatites during nappe emplacement at
10
11 531 *c.* 430-428 Ma (Ladenberger *et al.* 2014). The close correspondence of the age for this
12
13 532 migmatisation with the earliest Caledonian ages from the Fjørtoft gneiss encourages the
14
15 533 tentative proposal that migmatisation took place there, too, at that time. While this may
16
17 534 be true, the *c.* 430-428 Ma age for pegmatite intrusion at Åreskutan during Scandian
18
19 535 nappe emplacement corresponds closely to the evidence for growth of high-Ca garnet
20
21 536 rims in the Fjørtoft gneiss around 430-425 Ma (Holder *et al.* 2015), which we attribute to
22
23 537 partial melting. This suggests that partial melting of the Fjørtoft gneiss took place during
24
25 538 the earliest phase of exhumation of the far-western, Blåhø segment of the Seve Nappe
26
27 539 Complex. If two episodes of partial melting took place in these rocks (late Ordovician
28
29 540 and mid-Silurian), evidence must have been obscured by the subsequent intense ductile
30
31 541 shearing. If the Blåhø Nappe in western Norway can be directly correlated with the Seve
32
33 542 Nappe Complex in central Sweden, the evidence that the Blåhø Nappe, and possibly a
34
35 543 sheared pediment of Baltica basement orthogneisses, was still moving forelandwards
36
37 544 around 410 Ma suggest deformation at the base of the Åreskutan Nappe transferred to a
38
39 545 deeper structural level soon after *c.* 425 Ma.

40
41 546 The interpretations above, based on geological evidence and previous geochronological
42
43 547 studies, suggests that partial melting may have been significant in generating the zircon
44
45 548 U-Pb age pattern. If representative of the rock, the 447 Ma and 437-423 Ma zircon age
46
47 549 clusters probably represent discrete stages in which new zircon formed. This may have
48
49
50
51
52
53
54
55
56
57
58
59
60

1
2
3 550 involved complete neocrystallization and/or re-crystallisation of pre-existing zircon. The
4
5 551 latter is common in (U)HP granulites in other collisional orogens (e.g., Bröcker *et al.*
6
7 552 2010), as well as in ultra-high temperature (UHT-HT) rocks (e.g., Mezger & Krogstad,
8
9 553 1997; Kooijman *et al.* 2010), where partial melting was an important process. In the
10
11 554 Fjortoft rocks there was an apparent cessation in zircon crystallisation (or
12
13 555 neocrystallisation) during a period of *c.* 15 Ma, which also requires explanation.

14
15
16 556 Zircon crystallisation in felsic rocks can take place following an excursion beyond the
17
18 557 solidus (Yakymchuk & Brown, 2014), either by transient decompression or heating or
19
20 558 both. The following two options are hence proposed for the interpretation of the 447 and
21
22 559 437-423 Ma age clusters: (1) they postdate two distinct cycles of high-grade, possibly
23
24 560 kyanite-stable high temperature (HT) metamorphism - one before 447 Ma and the other
25
26 561 before 423 Ma; (2) they bracket two thermal excursions beyond, and back to, the solidus
27
28 562 during a single protracted stage of possibly kyanite-stable HT metamorphism. Regardless
29
30 563 of which of the two options proves true or which of these may be associated with micro-
31
32 564 diamond growth, the history and context of the rocks, as set out in the foregoing text,
33
34 565 requires at least one pulse of pre-Scandian metamorphism.

35
36
37 566 Previously published ages derived from the (U)HP eclogites in the Nordøyane and
38
39 567 adjacent region in the WGR, mainly in the range 415-400 Ma, are only represented in our
40
41 568 dataset by one concordant date of *c.* 415 Ma and a slightly discordant, similar date (Fig.
42
43 569 4b). The presence of Scandian UHP eclogites in the basal parts of the Blåhø Nappe in
44
45 570 Nordøyane (404.9 ± 7.9 Ma; Cutts & Smit, 2018) suggests that the Blåhø Nappe of
46
47 571 Fjortoft underwent Scandian, perhaps diamond-stable, UHP metamorphism. This
48
49 572 apparently resulted in very little new zircon growth or re-crystallisation in the sample
50
51
52
53
54
55
56
57
58
59
60

1
2
3 573 examined here. Scandian UHP eclogite formation in the allochthons and Baltica
4
5 574 basement evidently continued well after migmatization of the Blåhø metapelitic gneisses
6
7
8 575 such as those at Fjørtoft (there is evidence that gneisses in this area underwent partial
9
10 576 melting during UHP metamorphism; see e.g. Vrijmoed *et al.* 2013; Quas-Cohen, 2013).

11
12 577 The single concordant metamorphic zircon date at *c.* 396 Ma is identical within error with
13
14 578 a cluster of U-Th-Pb ages for matrix monazites in the Fjørtoft gneiss (Terry *et al.* 2000b).

15
16
17 579 This also closely corresponds to a regionally-distributed suite of titanite U-Pb ages
18
19 580 (Tucker *et al.* 1991) interpreted to date a widespread cessation of Pb loss during
20
21 581 exhumation of the WGR from below the major extensional Agdenes Detachment (Tucker
22
23 582 *et al.* 2004). The late horizontal lineation and sinistral shear fabric in northern Fjørtoft
24
25 583 may be attributed to this late-Scandian tectonism.

26
27
28 584 The zircon U-Pb dataset presented here demonstrates an early Caledonian, pre-Scandian
29
30 585 metamorphic event in the northwestern WGR that corresponds to a mid-Ordovician to
31
32 586 early Silurian subduction episode recorded in the main outcrop of the Seve Nappe. The
33
34 587 evidence for coeval Scandian UHP metamorphism of the Blåhø Nappe and in the Baltica
35
36 588 basement in Nordøyane (and probably more widely in the WGR) strongly suggests that
37
38 589 both underwent subduction in the late Silurian and early Devonian, and thus a ‘double-
39
40 590 dunk’ for the Blåhø-Seve Nappe of Fjørtoft.

41
42
43
44 591 The ‘double-dunk’ hypothesis (Brueckner & Van Roermund, 2004; Brueckner, 2006)
45
46 592 predicts both subduction and exhumation of a continental margin, so evidence is required for
47
48 593 an episode of exhumation of the subducted slab between any two ‘dunks’; if this is
49
50 594 lacking it is difficult to refute a single, prolonged subduction episode. In the WGR,
51
52 595 evidence for pre-Scandian tectonism and metamorphism has been effectively obliterated
53
54
55
56
57
58
59
60

1
2
3 596 by Scandian deformation and overprinting. All that can be deduced is that assembly of
4
5 597 the Middle Allochthon nappe stack and its emplacement onto the Baltica basement was
6
7 598 the earliest discernable event (e.g. Robinson *et al.* 2014). However, petrological evidence
9
10 599 for migmatisation during decompression in the correlative Åreskutan Nappe in the
11
12 600 foreland Seve Nappe Complex (Majka *et al.* 2012; Klonowska *et al.* 2014) shows that the
13
14 601 Seve Nappe did, at least partially, exhume following the Ordovician subduction event,
15
16 602 but before the Scandian subduction and climactic collision. The distribution of
17
18 603 concordant ages in our U-Pb zircon dataset, while showing clear clustering at specific
19
20 604 time intervals, does indicate some continuity of Caledonian zircon generation, which may
21
22 605 be due to incomplete exhumation after the first dunk and stalling at fairly deep, hot crustal
23
24 606 levels during the relatively brief interval before the Scandian dunk. Overall, the age
25
26 607 pattern from our new geochronological evidence for the Middle Allochthon within the
27
28 608 WGR is consistent with the predictions of the dunk tectonics model.

29
30
31 609 The sample from which our zircon set was separated has been iconic in UHP
32
33 610 metamorphic studies since the discovery of microdiamonds within it by Dobrzhinetskaya
34
35 611 *et al.* (1995), as this was the first metamorphic microdiamond find in the Caledonides and
36
37 612 one of the first globally. Yet, this sample remains enigmatic because no microdiamond
38
39 613 has yet been found *in-situ* within it. The demonstration of multiple metamorphic events in
40
41 614 this rock, of which two are probably **high- or ultrahigh- grade**, begs the question of the
42
43 615 genesis of the diamonds, although this is challenging because of their lack of
44
45 616 petrographic context. The possible double-dunk scenario for the Fjortoft gneiss set out
46
47 617 above **permits** that these rocks passed through diamond-stable physical conditions twice
48
49 618 during the Caledonian cycle. Hence, a priority for future work is to find the
50
51
52
53
54
55
56
57
58
59
60

1
2
3 619 microdiamonds *in-situ*, although several workers have already made great efforts to do
4
5 620 this. A possible barrier to success is the late structural-metamorphic overprint that this
6
7
8 621 belt of Blåhø has suffered, so future efforts might be better focused on adjacent areas
9
10 622 where this overprint is less complex and intense.

11
12 623 Finally, it is worth noting the comparison between the zircon dates presented above and
13
14 624 previously published monazite dates (Terry *et al.* 2000b; Holder *et al.* 2015; Liu &
15
16 625 Massonne, 2019), which reinforce the common observation that zircon and monazite age
17
18 626 records are complementary and that both only rarely provide the same age results, and
19
20 627 represent the same petrological process, in a single rock (Kooijman *et al.* 2017).
21
22
23
24 628

25 26 629 **7. Conclusions**

27
28 630 (1) The diamond-bearing gneiss from Fjørtoft in the Nordøyane UHP domain of the
29
30 631 Western Gneiss Region contains detrital zircon cores that reveal Baltic provenance.
31
32 632 This is consistent with previously proposed affinity of the studied gneiss to the Seve-
33
34 633 Blåhø Nappe of the Middle Allochthon. A few Archean ages are, however, clearly
35
36 634 exotic in respect to the local basement of the WGR directly underlying the studied
37
38 635 gneiss. Thus, a more exotic source is required for these zircons both at Fjørtoft and in
39
40 636 the other diamond-bearing gneisses of the Seve Nappe Complex.
41
42
43

44 637 (2) At least two distinct high-grade metamorphic events preceding the final stage of the
45
46 638 Scandian collision are recorded by the diamond-bearing gneiss from Fjørtoft: (1) at
47
48 639 446.6 ± 2.1 Ma; and (2) prolonged or multiple event(s) lasting from *c.* 437 to *c.* 423 Ma.
49
50 640 None of the above-mentioned ages can yet be unequivocally linked directly to UHP
51
52
53
54
55
56
57
58
59
60

1
2
3 641 metamorphism; they instead could represent P-T excursions related to episodes of
4
5 642 partial melting, each most likely following an episode of UHP metamorphism.
6

7
8 643 (3) The youngest obtained metamorphic zircon dates, scattering from *c.* 415 to *c.* 397 Ma
9
10 644 suggest a metamorphic overprint subsequent to the previous events, likely related to the
11
12 645 exhumation following final stages of the Scandian phase of the Baltica-Laurentia
13
14 646 collision, first of all by translation toward the foreland, then by motion on major west-
15
16 647 vergent detachments, but both relating to exhumation of Scandian UHP rocks.
17
18

19 648 (4) Multiple zircon growth events recorded in the Fjørtoft gneiss reflect its complicated
20
21 649 and protracted metamorphic evolution. It is inferred that such complex metamorphic
22
23 650 zircon ages pattern resulted from several subduction-exhumation cycles, as predicted by
24
25 651 the dunk tectonics model for the Scandinavian Caledonides.
26
27

28 652 (5) The data are consistent with predictions of the dunk tectonics model, indicating that it
29
30 653 provides a plausible explanation for the development of a major part of the
31
32 654 Scandinavian Caledonides.
33
34

35 655

36 37 38 656 **Acknowledgements**

39
40 657 We thank Melanie Schmitt for her assistance with the laser ablation analysis. Hannes
41
42 658 Brueckner and David Young are acknowledged for their helpful reviews. KW, SC and
43
44 659 JM were supported by the National Science Centre (Poland) CALSUB project no.
45
46 660 2014/14/E/ST10/00321. This is Vegacenter publication #016.
47
48

49 661

50 51 662 **Declaration of Interest**

52
53 663 None
54
55
56
57
58
59
60

1
2
3 664
4

5 665 **References**
6

7
8 666 Andersen, T. B., Jamtveit, B., Dewey, J. F. & Swensson, E. 1991. Subduction and
9
10 667 eduction of continental crust: major mechanisms during continent–continent collision and
11
12 668 orogenic extensional collapse, a model based on the south Norwegian Caledonides. *Terra*
13
14 669 *Nova* **3**, 303–310. <http://dx.doi.org/10.1111/j.1365-3121.1991.tb00148.x>.
15

16
17 670

18
19 671 Barnes, C., Majka, J., Schneider, D. A., Walczak, K., Bukala, M. & Kościńska, K.,
20
21 672 2019. High-spatial resolution dating of zircon and monazite reveals late Cambrian
22
23 673 subduction of the Vaimok Lens of the Seve Nappe Complex in the Scandinavian
24
25 674 Caledonides of Sweden, *Contributions to Mineralogy and Petrology*, in press,
26
27 675 <https://doi.org/10.1007/s00410-018-1539-1>.
28
29

30
31 676

32
33 677 Bingen, O. & van Breemen, O. 1998. Tectonic regimes and terrane boundaries in the high
34
35 678 grade Sveconorwegian belt of SW Norway, inferred from U-Pb zircon geochronology
36
37 679 and geochemical signature of augen gneiss suites. *Journal of the Geological Society*,
38
39 680 *London* **155**, 143–154.
40

41
42 681

43
44 682 Bingen, B., Davis, W. J. & Austrheim, H. 2001. Zircon U-Pb geochronology in the
45
46 683 Bergen arc eclogites and their Proterozoic protoliths, and implications for the pre-
47
48 684 Scandian evolution of the Caledonides in western Norway, *Geological Society of*
49
50 685 *America Bulletin* **113**, 640–649.
51

52
53
54 686
55
56
57
58
59
60

- 1
2
3 687 Bingen, B. & Solli, A. 2009. Geochronology of magmatism in the Caledonian and
4
5 688 Sveconorwegian belts of Baltica: synopsis for detrital zircon provenance studies.
6
7 689 *Norwegian Journal of Geology* **89**, 267-290
8
9
10 690
11
12 691 Black, L. P., Kamo, S. L. , Allen, C. M., Davis, D. W., Aleinikoff, J. N., Valley, J. W.,
13
14 692 Mundil, R., Campbell, I. H., Korsch, R. J., Williams, I. S. & Foudoulis, C. 2004.
15
16 693 Improved $^{206}\text{Pb}/^{238}\text{U}$ microprobe geochronology by the monitoring of a
17
18 694 trace-element-related matrix effect; SHRIMP, ID-TIMS, ELA-ICP-MS and oxygen
19
20 695 isotope documentation for a series of zircon standards, *Chemical Geology* **205** (1-2),
21
22 696 115-140.
23
24
25 697
26
27 698 Bröcker, M., Klemd, R., Kooijman, E., Berndt, J. & Larinov, A. 2010. Zircon
28
29 699 geochronology and trace element characteristics of eclogites and granulites from the
30
31 700 Orlica-Śnieżnik complex, Bohemian Massif. *Geological Magazine* **147**, 339-362.
32
33
34 701
35
36 702 Brueckner, H.K., 2006. Dunk, dunkless and re-dunk tectonics: a model for
37
38 703 metamorphism, lack of metamorphism, and repeated metamorphism of HP/UHP terranes.
39
40
41 704 *International Geology Review* **48**/11, 978-995.
42
43
44 705
45
46 706 Brueckner, H. K., Carswell, D. A., Griffin, W. L., Medaris L. G. Jr., Van Roermund, H.
47
48 707 L. M., & Cuthbert, S. J. 2010. The mantle and crustal evolution of two garnet peridotite
49
50 708 suites from the Western Gneiss Region, Norwegian Caledonides: An isotopic
51
52 709 investigation. *Lithos* **117**, 1-19.
53
54
55
56
57
58
59
60

1
2
3 710
4

5 711 Brueckner, H. K. & van Roermund, H. L. M. 2004. Dunk tectonics: a multiple
6
7 712 subduction/ eduction model for the evolution of the Scandinavian Caledonides. *Tectonics*
8
9 713 **23**, TC2004, [doi:10.1029/2003TC001502](https://doi.org/10.1029/2003TC001502).

10
11
12 714

13
14 715 Brueckner, H. K., van Roermund, H. L. M. & Pearson, N. J. 2004. An Archean(?) to
15
16 716 Paleozoic evolution for garnet peridotite lens with sub-Baltic Shield affinity within the
17
18 717 Seve Nappe Complex of Jämtland, Sweden, Central Scandinavian Caledonides. *Journal*
19
20 718 *of Petrology* **45** (2), 415–437. [https://doi.org/10.1093/](https://doi.org/10.1093/petrology/egg088)
21
22
23

24 719

25
26 720 Brueckner, H. K. & van Roermund, H. L. M. 2007. Concurrent HP metamorphism on
27
28 721 both margins of Iapetus: Ordovician ages for eclogites and garnet pyroxenites from the
29
30 722 Seve Nappe Complex, Swedish Caledonides. *Journal of the Geological Society, London*
31
32 723 **164**, 117–128.

33
34
35 724

36
37 725 Brueckner, H. K. & Cuthbert, S. J. 2013. Extension, disruption, and translation of an
38
39 726 orogenic wedge by exhumation of large ultrahigh-pressure terranes: Examples from the
40
41 727 Norwegian Caledonides. *Lithosphere* **5** (3), 277–289.

42
43
44 728

45
46 729 Bukała, M., Klonowska, I., Barnes, C., Majka, J., Kościńska, K., Janák, M., Fassmer, K.,
47
48 730 Broman, C. & Luptáková, J. 2018. UHP metamorphism recorded by phengite eclogite
49
50 731 from the Caledonides of northern Sweden: P–T path and tectonic implications. *Journal of*
51
52 732 *Metamorphic Geology* **36**, 529–545 <https://doi.org/10.1111/jmg.12306>.

53
54
55
56
57
58
59
60

1
2
3 733
4

5 734 Butler, J. P., Jamieson, R. A. Steenkamp, H. M. & Robinson, P. 2013. Discovery of
6
7 735 coesite–eclogite from the Nordøyane UHP domain, Western Gneiss Region, Norway:
8
9 736 field relations, metamorphic history, and tectonic significance. *Journal of Metamorphic*
10
11 737 *Geology* **31**, 147–163.
12
13

14 738
15

16
17 739 Carswell, D. A. & van Roermund H. L. M. 2005. On multi-phase mineral inclusions
18
19 740 associated with microdiamond formation in mantle-derived peridotite lens at Bardane on
20
21 741 Fjærtøft, west Norway. *European Journal of Mineralogy* **17**, 31–42.
22
23

24 742
25

26 743 Carswell, D. A., Van Roermund, H. L. M. & Wiggers Devries, D. F. 2006. Scandian
27
28 744 Ultrahigh-Pressure Metamorphism of Proterozoic Basement Rocks on Fjærtøft and Otrøy,
29
30 745 Western Gneiss Region, Norway. *International Geology Review* **48**, 957–977.
31
32

33 746
34

35 747 Cawood, P.A., Strachan, R., Cutts, K., Kinny, P.D., Hand, M. & Pisarevsky, S. 2010.
36
37 748 Neoproterozoic orogeny along the margin of Rodinia: Valhalla orogen, North Atlantic.
38
39 749 *Geology* **38**, 99–102.
40
41

42 750
43

44 751 Corfu, F. & Andersen, T. B. 2002. U-Pb ages of the Dalsfjord complex, SW Norway, and
45
46 752 their bearing on the correlation of allochthonous crystalline segments of the Scandinavian
47
48 753 Caledonides: *International Journal of Earth Sciences* **91**, p. 955–963,
49
50 754 doi:10.1007/s00531-002-0298-3.
51
52

53 755
54
55
56
57
58
59
60

1
2
3 756 Cuthbert, S. J., Harvey, M. A. & Carswell, D. A. 1983. A tectonic model for the
4
5 757 metamorphic evolution of the Basal Gneiss Complex, western South Norway: *Journal of*
6
7 758 *Metamorphic Geology* **1**, p. 63–90, doi:10.1111/j.1525-1314.1983.tb00265.x.
8
9

10 759

11
12 760 Cuthbert, S. J., Carswell, D. A., Krogh-Ravna, E. J. & Wain, A. 2000. Eclogites and
13
14 761 eclogites in the Western Gneiss Region, Norwegian Caledonides. *Lithos* **52**, 165–195.
15
16 762 [http://dx.doi.org/10.1016/S0024-4937\(99\)00090-0](http://dx.doi.org/10.1016/S0024-4937(99)00090-0).
17
18

19 763

20
21 764 Cutts, J.A. & Smit, M.A. 2018, Rates of deep continental burial from Lu-Hf garnet
22
23 765 chronology and Zr-in-rutile thermometry on (ultra-)high pressure rocks. *Tectonics* **37**, 71-
24
25 766 88 doi: 10.1002/2017TC004723.
26
27

28 767

29
30
31 768 DesOrmeau, J. W., Gordon, S. M., Kylander-Clark, A. R. C., Hacker, B. R., Bowring, S.
32
33 769 A., Schoene, B. & Samperton, K. M. 2015. Insights into (U)HP metamorphism of the
34
35 770 Western Gneiss Region, Norway: a high-spatial resolution and high-precision zircon
36
37 771 study. *Chemical Geology* **414**, 138–155.
38
39

40 772

41
42 773 Dobrzhinetskaya, L., Eide, E. A., Larsen, R. B., Sturt, B. A., Trønnes, R. G., Smith, D.
43
44 774 C., Taylor, W. R. & Posukhova, T. V. 1995. Microdiamond in high-grade metamorphic
45
46 775 rocks of the Western Gneiss Region, Norway: *Geology* **23**, p. 597–600.
47
48

49 776

50
51 777 Emmett, T. 1996. The provenance of pre-Scandian continental flakes within the
52
53 778 Caledonide orogen of south-central Norway, in *Precambrian Crustal Evolution in the*
54
55
56
57
58
59
60

- 1
2
3 779 *North Atlantic Region* (Brewer, T. S., ed.), pp. 359-366. Geological Society of London
4
5 780 Special Publication no. 112.
6
7 781
8
9
10 782 Fassmer, K., Klonowska, I., Walczak, K., Andersson, B., Froitzheim, N., Majka, J.,
11
12 783 Fonseca, R. O. C., Münker, C., Janák, M. & Whitehouse, M. 2017. Middle Ordovician
13
14 784 subduction of continental crust in the Scandinavian Caledonides: an example from
15
16 785 Tjeliken, Seve Nappe Complex, Sweden. *Contribution to Mineralogy and Petrology* **172**,
17
18 786 103, <https://doi.org/10.1007/s00410-017-1420-7>.
19
20
21 787
22
23 788 Gaál, G. & Gorbastshev, R. 1991. An Outline of the precambrian evolution of the baltic
24
25 789 shield. *Precambrian Research* **35**, 15-52.
26
27
28 790
29
30 791 Gee, D.G. 1980. Basement–cover relationships in the central Scandinavian Caledonides.
31
32 792 *Geologiska Föreningens i Stockholm Förhandlingar* **102**, p. 455–474,
33
34 793 <https://doi.org/10.1080/11035898009454500>.
35
36
37 794
38
39 795 Gee, D. G., Juhlin, C., Pascal, C. & Robinson, P. 2010. Collisional Orogeny in the
40
41 796 Scandinavian Caledonides (COSC). *Geologiska Föreningens i Stockholm Förhandlingar*
42
43 797 **132**, 29–44.
44
45
46 798
47
48 799 Gee, D. G., Janák, M., Majka, J., Robinson, P. & van Roermund, H. 2013. Subduction
49
50 800 along and within the Baltoscandian margin during closing of the Iapetus Ocean and
51
52 801 Baltica–Laurentia collision. *Lithosphere* **5**, 169–178.
53
54
55
56
57
58
59
60

1
2
3 802
4

5 803 Gee, D. G., Ladenberger, A., Dahlqvist, P., Majka, J., Be'eri-Shlevin, Y., Frei, D. &
6
7 804 Thomsen, T. 2014. The Baltoscandian margin detrital zircon signatures of the central
8
9 805 Scandes. In: *New Perspectives on the Caledonides of Scandinavia and Related Areas* (eds
10
11 806 Corfu, F., Gasser, D. & Chew, D. M.), pp. 131–155. Geological Society, London, Special
12
13 807 Publications no. 390.
14
15

16
17 808

18
19 809 Gee, D. G., Andréasson, P.-G., Lorenz, H., Frei, D. & Majka, J. 2015. Detrital zircon
20
21 810 signatures of the Baltoscandian margin along the Arctic Circle Caledonides in Sweden:
22
23 811 The Sveconorwegian connection. *Precambrian Research* **256**, 40-56.
24
25

26
27 812

28
29 813 Gordon, S. M., Whitney, D. L., Teyssier, C., Fossen, H. & Kylander-Clark, A. R. C.
30
31 814 2016. Geochronology and geochemistry of zircon from the northern Western Gneiss
32
33 815 Region: Insights into the Caledonian tectonic history of western Norway. *Lithos* **246-247**,
34
35 816 134-148.
36
37

38
39 817

40 818 Griffin, W. L. & Brueckner, H. K. 1985. REE, Rb–Sr and Sm–Nd studies of Norwegian
41
42 819 eclogites. *Chemical Geology* **52**, 249–271. [http://dx.doi.org/10.1016-](http://dx.doi.org/10.1016/0168-9622(85)90021-1)
43
44 820 [9622\(85\)90021-1](http://dx.doi.org/10.1016/0168-9622(85)90021-1).
45
46

47 821

48
49 822 Grimmer, J. C., Glodny, J., Drüuppel, K., Greiling, R. O. & Kontny, A. 2015. Early- to
50
51 823 mid-Silurian extrusion wedge tectonics in the central Scandinavian Caledonides. *Geology*
52
53 824 **43**, 347–350.
54
55
56
57
58
59
60

1
2
3 825
4

5 826 Hacker, B. R. & Gans, P. B. 2005. Continental collisions and the creation of ultrahigh-
6
7 827 pressure terranes: petrology and thermochronology of nappes in the central Scandinavian
8
9 828 Caledonides. *Geological Society of America Bulletin* **117**, 117–134.
10
11
12 829 <http://dx.doi.org/10.1130/B25549.1>.
13

14 830

15
16
17 831 Hacker, B. R., Andersen, T. B., Johnston, S., Kylander-Clark, A. R. C., Peterman, E. M.,
18
19 832 Walsh, E. O. & Young, D. 2010. High-temperature deformation during continental-
20
21 833 margin subduction and exhumation: the ultrahigh-pressure Western Gneiss Region of
22
23 834 Norway. *Tectonophysics* **480** (1–4), 149–171.
24
25
26 835 <http://dx.doi.org/10.1016/j.tecto.2009.08.012>.
27

28 836

29
30
31 837 Hacker, B. R., Kylander-Clark, A. R. C., Holder, R., Andersen, T. B., Peterman, E. M.,
32
33 838 Walsh, E. O. & Munnikhuis, J. K. 2015. Monazite response to ultrahigh-pressure
34
35 839 subduction from U–Pb dating of laser ablation split stream. *Chemical Geology* **409**, 28–
36
37 840 41.
38

39 841

40
41
42 842 Holder, R. M., Hacker, B. R., Kylander-Clark, A. R. C. & Cottle, J. M. 2015. Monazite
43
44 843 trace-element and isotopic signatures of (ultra)high-pressure metamorphism: examples
45
46 844 from the Western Gneiss Region, Norway. *Chemical Geology* **409**, 99–111.
47
48

49 845
50
51
52
53
54
55
56
57
58
59
60

1
2
3 846 Jackson, S.E., Pearson, N.J., Griffin, W.L. & Belousova, E.A. 2004. The application of
4
5 847 laser ablation-inductively coupled plasma-mass spectrometry to in situ U-Pb zircon
6
7 848 geochronology. *Chemical Geology* **211**, 47–69.

9
10 849

11
12 850 Jamtveit, B., Carswell, D.A. & Mearns, E.W. 1991. Chronology of the high-pressure
13
14 851 metamorphism of Norwegian garnet peridotites/pyroxenites. *Journal of Metamorphic*
15
16 852 *Geology* **9**, 125-139.

17
18
19 853

20
21 854 Janák, M., van Roermund, H., Majka, J. & Gee, D. 2013. UHP metamorphism recorded
22
23 855 by kyanite-bearing eclogite in the Seve Nappe Complex of northern Jämtland, Swedish
24
25 856 Caledonides. *Gondwana Research* **23**, 865-879.

26
27
28 857

29
30 858 Kirkland, C. L., Daly, J. S. & Whitehouse, M. J. 2006. Granitic magmatism of
31
32 859 Grenvillian and late Neoproterozoic age in Finnmark, Arctic Norway—Constraining pre-
33
34 860 Scandian deformation in the Kalak Nappe Complex. *Precambrian Research* **145**, 24–52.

35
36
37 861

38
39 862 Klonowska, I., Janák, M., Majka, J., Froitzheim, N. & Kościńska, K. 2016. Eclogite and
40
41 863 garnet pyroxenite from Stor Jougdan, Seve Nappe Complex, Sweden: implications for
42
43 864 UHP metamorphism of allochthons in the Scandinavian Caledonides. *Journal of*
44
45 865 *Metamorphic Geology* **34**, 103–119.

46
47
48 866

49
50 867 Klonowska, I., Majka, J., Janak, M., Gee, D.G. & Ladenberger, A. 2014. Pressure –
51
52 868 temperature evolution of a kyanite – garnet polytic gneiss from Areskutan: evidence of
53
54
55
56
57
58
59
60

1
2
3 869 ultra-high-pressure metamorphism of the Seve Nappe Complex, west-central Jamtland,
4
5 870 Swedish Caledonides. In *New Perspectives on the Caledonides of Scandinavia and*
6
7 871 *Related Areas* (Corfu, F., Gasser, D. & Chew, D. M. eds), pp. 321-336. Geological
8
9 872 Society of London, Special Publications no. 390, <http://dx.doi.org/10.1144/SP390.7>.

11
12 873

13
14 874 Klonowska, I., Janák, M., Majka, J., Petrik, I., Froitzheim, N., Gee, D.G. & Sasinková,
15
16 875 V. 2017. Microdiamond on Åreskutan confirms regional UHP metamorphism in the Seve
17
18 876 Nappe Complex of the Scandinavian Caledonides. *Journal of Metamorphic Geology* **35**,
19
20 877 541–564.

21
22 878

23
24 879 Kooijman, E., Upadhyay, D., Mezger, K., Raith, M.M., Berndt, J. & Srikantappa, C.
25
26 880 2011. Response of the U–Pb chronometer and trace elements in zircon to ultrahigh-
27
28 881 temperature metamorphism: The Kadavur anorthosite complex, southern India. *Chemical*
29
30 882 *Geology* **290**, 177-188.

31
32 883

33
34 884 Kooijman, E., Berndt, J. & Mezger, K. 2012. U-Pb dating of zircon by laser ablation ICP-
35
36 885 MS: recent improvements and new insights. *European Journal of Mineralogy* **24** (1), 5-
37
38 886 21.

39
40 887

41
42 888 Kooijman, E., Smit, M. A., Ratschbacher, L. & Stearns, M. A. 2017. A view into crustal
43
44 889 evolution at mantle depths. *Earth and Planetary Science Letters* **465**, 59-69.

45
46 890

47
48

49
50

51
52

53
54

55
56

57
58
59
60

1
2
3 891 Krill, A. G. 1980. Tectonics of the Oppdal area, central Norway. *Geologiska Föreningens*
4
5 892 *i Stockholm Förhandlingar* **102**, 523–530.

6
7
8 893

9
10 894 Krill, A. G. 1985. Relationship between the western gneiss region and the Trondheim
11
12 895 region: Stockwerk tectonics reconsidered. In *The Caledonide Orogen – Scandinavia and*
13
14 896 *Related Areas* (Gee, D. G. & Sturt, B. A. eds) pp. 475–483. John Wiley and Sons,
15
16 897 Chichester.

17
18
19 898

20
21 899 Krogh, E. J. 1977. Evidence for Precambrian continent–continent collision in western
22
23 900 Norway. *Nature* **267**, 17–19. <http://dx.doi.org/10.1038/267017a0>.

24
25
26 901

27
28 902 Krogh, T. E., Kamo, S. L., Robinson, P., Terry, M. P. & Kwok, K. 2011. U–Pb zircon
29
30 903 geochronology of eclogites from the Scandian Orogen, northern Western Gneiss Region,
31
32 904 Norway: 14–20 million years between eclogite crystallization and return to amphibolite-
33
34 905 facies conditions. *Canadian Journal of Earth Sciences* **48**, 441–472.
35
36 906 <http://dx.doi.org/10.1139/E10-076>.

37
38
39 907

40
41
42 908 Kylander-Clark, A. R. C., Hacker, B. R. & Mattinson, J.M. 2008. Slow exhumation of
43
44 909 UHP terranes: titanite and rutile ages of the Western Gneiss Region, Norway. *Earth and*
45
46 910 *Planetary Science Letters* **272** (3–4), 531–540.
47
48 911 <http://dx.doi.org/10.1016/j.epsl.2008.05.019>.

49
50
51 912
52
53
54
55
56
57
58
59
60

1
2
3 913 Kylander-Clark, A. R. C., Hacker, B. R., Johnson, C. M., Beard, B. L. & Mahlen, N. J.
4
5 914 2009. Slow subduction of a thick ultrahigh-pressure terrane. *Tectonics* **28**, TC2003,
6
7 915 doi:10.1029/2007TC002251.
8
9

10 916

11
12 917 Labrousse, L., Jolivet, L., Agard, P., Hebert, R. & Andersen, T. B. 2002. Crustal-scale
13
14 918 boudinage and migmatization of gneiss during their exhumation in the UHP Province of
15
16
17 919 Western Norway. *Terra Nova* **14**, 263–270, 2002.
18

19 920

20
21 921 Ladenberger, A., Be'eri-Shlevin, Y., Claesson, S., Gee, D. G., Majka, J. & Romanova, I.
22
23 922 V. 2014. Tectonometamorphic evolution of the Åreskutan Nappe-Caledonian history
24
25 923 revealed by SIMS U–Pb zircon geochronology. In *New perspectives on the Caledonides*
26
27 924 *of Scandinavia and Related Areas* (Corfu, F., Gasser, D. & Chew, D.M. eds) pp. 337-368.
28
29 925 Geological Society of London, Special Publications no. 390.
30
31

32 926

33
34
35 927 Larsen, R. B., Eide, E. A., & Burke, A. J. 1998. Evolution of metamorphic volatiles
36
37 928 during exhumation of microdiamond-bearing granulites in the Western Gneiss Region,
38
39 929 Norway. *Contributions to Mineralogy and Petrology* **133**, 106-121.
40
41

42 930

43
44 931 Liu, P. & Massone, H.-J. 2019. An anticlockwise P-T-t path at high-pressure, high-
45
46 932 temperature conditions for a migmatitic gneiss from the island of Fjørtoft, Western
47
48 933 Gneiss Region, Norway, indicates two burial events during the Caledonian orogeny.

49
50 934 *Journal of Metamorphic Geology*, <https://doi.org/10.1111/jmg.12476>.
51
52

53 935
54
55
56
57
58
59
60

1
2
3 936 Ludwig, K. R. 2012. User's Manual for Isoplot 3.75 a Geochronological Toolkit for
4
5 937 Microsoft Excel. Berkeley Geochronology Center Special Publication no. 5. Downloaded
6
7
8 938 at: http://www.bgc.org/isoplot_etc/isoplot.html 2015-02-06.

9
10 939

11
12 940 Majka, J., Be'eri-Shlevin, Y., Gee, D. G., Ladenberger, A., Claesson, S., Konecny, P. &
13
14 941 Klonowksa, I. 2012. Multiple monazite growth in the Åreskutanmigmatite: evidence for a
15
16 942 polymetamorphic Late Ordovician to Late Silurian evolution in the Seve Nappe Complex
17
18 943 of west-central Jämtland, Sweden. *Journal of Geosciences* **57**, 3–2.

19
20
21 944

22
23 945 Majka, J., Rosén, Å., Janák, M., Froitzheim, N., Klonowska, I., Manecki, M., Sasinková,
24
25 946 V. & Yoshida, K. 2014. Microdiamond discovered in the Seve Nappe (Scandinavian
26
27 947 Caledonides) and its exhumation by the “vacuum-cleaner” mechanism. *Geology* **42**,
28
29 948 1107–1110.

30
31
32 949

33
34 950 Medaris, L. G., Brueckner, H. K., Cai, Y., Griffin W. L., Janák, M. 2018. Eclogites in
35
36 951 peridotite massifs in the Western Gneiss Region, Scandinavian Caledonides: Petrogenesis
37
38 952 and comparison with those in the Variscan Moldanubian Zone. *Lithos* **322**, 352-346.

39
40
41 953

42
43 954 Mezger, K. & Krogstad, E. J. 1997. Interpretation of discordant U–Pb zircon ages: an
44
45 955 evaluation. *Journal of Metamorphic Geology* **15**, 127-140.

46
47
48 956

49
50
51

52
53
54

55
56
57

58
59
60

- 1
2
3 957 Mørk, M. B. E., Kullerud, K. V. & Stabel, A. 1988. Sm–Nd dating of Seve eclogites,
4
5 958 Norrbotten, Sweden-evidence for early Caledonian (505 Ma) subduction. *Contributions*
6
7 959 *to Mineralogy and Petrology* **99**, 344–351.
8
9
10 960
11
12 961 Norton, M.G. 1991. The Nordfjord-Sogn Detachment, W. Norway. *Norsk Geologisk*
13
14 962 *Tidsskrift* **67**, pp. 93-106.
15
16
17 963
18
19 964 Paulsson, O. & Adréasson, P. G. 2002. Attempted break-up of Rodinia at 850 Ma:
20
21 965 geochronological evidence from the Seve–Kalak Superterrane, Scandinavian
22
23 966 Caledonides. *Journal of the Geological Society, London* **159**, 751–761.
24
25
26 967
27
28 968 Quas-Cohen, A. 2013. Norwegian orthopyroxene eclogites: petrogenesis and implications
29
30 969 for metasomatism and crust-mantle interactions during subduction of continental crust.
31
32 970 Unpublished PhD thesis, University of Manchester.
33
34
35 971
36
37 972 Roberts, R. J., Corfu, F., Torskvik, T. H., Hetherington, C. J. & Ashwal, L. D. 2010. Age
38
39 973 of alkaline rocks in the Seiland Igneous Province, Northern Norway. *Journal of the*
40
41 974 *Geological Society, London* **167**, 71-81.
42
43
44 975
45
46 976 Robinson, P. 1995. Extension of Trollheimen tectonostratigraphic sequence in deep
47
48 977 synclines near Molde and Brattvåg, Western Gneiss Region, southern Norway. *Norsk*
49
50 978 *Geologisk Tidsskrift* **75**, 181–197.
51
52
53 979
54
55
56
57
58
59
60

- 1
2
3 980 Robinson, P, Langenhorst, F. & Terry, M. P. 2003. Interpretation of inclusions in
4
5 981 kyanite-garnet gneiss: Fjørtoft, Western Norway. Alice Wain Eclogite Field Symposium,
6
7 982 Selje, West Norway. Abstract Volume, Norges geologiske undersøkelse Report No.
8
9 983 2003.055,119-120.
10
11
12 984
13
14 985 Robinson, P. & Hollocher, K. 2008. Geology of Trollheimen. In: Robinson, P., Roberts,
15
16 986 D., Gee, D. G. (Eds.), Guidebook: a tectonostratigraphic transect across the central
17
18 987 Scandinavian Caledonides. NGU report 2008.064, pt. II. Geological Survey of Norway,
19
20 988 Trondheim, pp. 6-1–6-7.
21
22
23 989
24
25 990 Robinson, P., Roberts, D., Gee, D. G. & Solli, A. 2014. A major synmetamorphic Early
26
27 991 Devonian thrust and extensional fault system in the mid-Norway Caledonides: relevance
28
29 992 to exhumation of HP and UHP rocks. In *New Perspectives on the Caledonides of*
30
31 993 *Scandinavia and Related Areas* (Corfu, F., Gasser, D. & Chew, D. M. eds) pp. 241-270.
32
33 994 Geological Society of London, Special Publications no. 390.
34
35
36 995
37
38 996 Røhr, T. S., Corfu, F., Austrheim, H. & Andersen, T. B. 2004. Sveconorwegian U-Pb
39
40 997 zircon and monazite ages of granulite-facies rocks, Hisarøya, Gulen, Western Gneiss
41
42 998 Region, Norway. *Norwegian Journal of Geology* **84**, 251-256.
43
44
45 999
46
47
48
49 1000 Root, D. B., Hacker, B. R., Gans, P. B., Ducea, M. N., Eide, E. A. & Mosenfelder, L.
50
51 1001 2005. Discrete ultrahigh-pressure domains in the Western Gneiss Region, Norway:
52
53
54
55
56
57
58
59
60

- 1
2
3 1002 Implications for formation and exhumation. *Journal of Metamorphic Geology* **23**, (1), p.
4
5 1003 45–61, doi:10.1111/j.1525-1314.2005.00561.x.
6
7 1004
8
9
10 1005 Root, D. & Corfu, F. 2012. U–Pb geochronology of two discrete Ordovician high-
11
12 1006 pressure metamorphic events in the Seve Nappe Complex, Scandinavian Caledonides.
13
14 1007 *Contributions to Mineralogy and Petrology* **163**, 769–788.
15
16 1008
17
18
19 1009 Scambelluri M., van Roermund H. L. M. & Pettke T. 2010. Mantle wedge peridotites:
20
21 1010 Fossil reservoirs of deep subduction zone processes: Inferences from high and ultrahigh-
22
23 1011 pressure rocks from Bardane (Western Norway) and Ulten (Italian Alps). *Lithos* **120**,
24
25 1012 186-201.
26
27
28 1013
29
30
31 1014 Sláma J., Košler J., Condon D. J., Crowley J. L., Gerdes A., Hanchar J. M., Horstwood
32
33 1015 M. S. A., Morris G. A., Nasdala L., Norberg N., Schaltegger U., Schoene B., Tubrett M.
34
35 1016 N. & Whitehouse M. J. 2008. Plešovice zircon — A new natural reference material for
36
37 1017 U–Pb and Hf isotopic microanalysis. *Chemical Geology* **249**, 1-35.
38
39 1018
40
41
42 1019 Smit, M. A., Scherer, E. E., Bröcker, M. & van Roermund, H. L. M. 2010, Timing of
43
44 1020 eclogite facies metamorphism in the southernmost Scandinavian Caledonides by Lu–Hf
45
46 1021 and Sm–Nd geochronology. *Contributions to Mineralogy and Petrology* **159**, 521-539.
47
48 1022
49
50
51 1023 Smit, M. A., Bröcker, M., Kooijman, E., & Scherer, E. E. 2011. Provenance and
52
53 1024 exhumation of an exotic eclogite-bearing nappe in the Caledonides: a U–Pb and Rb–Sr
54
55
56
57
58
59
60

- 1
2
3 1025 study of the Jæren nappe, SW Norway. *Journal of the Geological Society London* **168**,
4
5 1026 421-439.
6
7 1027
8
9
10 1028 Stephens, M. B. & Gee, D. G. 1985. A tectonic model for the evolution of the eugeoclinal
11
12 1029 terranes in the central Scandinavian Caledonides. In *The Caledonide Orogen—*
13
14 1030 *Scandinavia and Related Areas*, (eds D. G. Gee & G. A. Sturt), pp. 953 – 978, John
15
16 1031 Wiley, Hoboken, N.J.
17
18
19 1032
20
21 1033 Stephens, M. 1988. The Scandinavian Caledonides; a complexity of collisions. *Geology*
22
23 1034 *Today* **4**, 20–24.
24
25
26 1035
27
28 1036 Stephens, M. B. & Gee, D. G. 1989. Terranes and polyphase accretionary history in the
29
30 1037 Scandinavian Caledonides, in *Terranes in the Circum-Atlantic Paleozoic Orogens* (ed R.
31
32 1038 D. Dallmeyer) pp. 17-30, Geological Society of America, Special Papers no. 230.
33
34
35 1039
36
37 1040 Terry, M. P., Robinson P., Hamilton, M. A. & Jercinovic, M. J. 2000. Monazite
38
39 1041 geochronology of UHP and HP metamorphism, deformation and exhumation,
40
41 1042 Nordøyane, Western Gneiss Region, Norway, *American Mineralogist* **85**, 1651 – 1664.
42
43
44 1043
45
46 1044 Terry, M. P., Robinson, P. & Ravna, E. J. K. 2000. Kyanite eclogite thermobarometry
47
48 1045 and evidence for thrusting of UHP over HP metamorphic rocks, Nordøyane, Western
49
50 1046 Gneiss Region, Norway. *American Mineralogist* **85**, 1637–1650.
51
52
53 1047
54
55
56
57
58
59
60

- 1
2
3 1048 Terry, M. P. & Robinson, P. 2004. Geometry of eclogite facies structural features;
4
5 1049 implications for production and exhumation of ultrahigh-pressure and high-pressure
6
7 1050 rocks, Western Gneiss region, Norway. *Tectonics* **23**, 1–23.
8
9
10 1051
11
12 1052 Tucker, R. D., Boyd, R. & Barnes, S.-J. 1990. A U–Pb zircon age for the Råna intrusion,
13
14 1053 N. Norway: New evidence of basic magmatism in the Scandinavian Caledonides in Early
15
16 1054 Silurian time. *Norsk Geologisk Tidsskrift* **70**, 229–239.
17
18
19 1055
20
21 1056 Tucker, R. D., Krogh, T. E. & Råheim, A. 1991. Proterozoic evolution and age-province
22
23 1057 boundaries in the central parts of the Western Gneiss Region, Norway: Results of U-Pb
24
25 1058 dating of accessory minerals from Trondheimsfjord to Geiranger, in *Mid-Proterozoic*
26
27 1059 *Laurentia-Baltica*, edited by C. F. Gower, T. Rivers, and B. Ryan, The Geological
28
29 1060 Association of Canada Special Papers, **38**, 149 – 173.
30
31
32 1061
33
34 1062 Tucker, R. D., Robinson, P., Solli, A., Gee, D. G., Thorsnes, T., Krogh, T. E., Nordgulen,
35
36 1063 Ø. & Bickford, M.E. 2004. Thrusting and extension in the Scandian hinterland, Norway:
37
38 1064 New U–Pb ages and tectonostratigraphic evidence. *American Journal of Science* **304** (6),
39
40 1065 477–532. <http://dx.doi.org/10.2475/ajs.304.6.477>.
41
42
43 1066
44
45 1067 Vrijmoed, J., Van Roermund, H. & Davies, G. 2006. Evidence for diamond-grade ultra-
46
47 1068 high pressure metamorphism and fluid interaction in the Svartberget Fe–Ti garnet
48
49 1069 peridotite–websterite body, Western Gneiss Region, Norway. *Mineralogy and Petrology*
50
51 1070 **88**, 381-405.
52
53
54
55
56
57
58
59
60

- 1
2
3 1071
4
5 1072 Vrijmoed, J. C., Austrheim, H., John, T., Hin, R. C., Corfu, F. & Davies, G. R. 2013.
6
7 1073 Metasomatism in the ultrahigh-pressure Svartberget garnet-peridotite (Western Gneiss
8
9 1074 Region, Norway): Implications for the transport of crust-derived fluids within the mantle.
10
11 1075 *Journal of Petrology* **54**, 1815-1848.
12
13 1076
14
15 1077 Walker, S., Thirlwall, M. F., Strachan, R. A. & Bird, A. F. 2016. Evidence from Rb–Sr
16
17 1078 mineral ages for multiple orogenic events in the Caledonides of Shetland, Scotland.
18
19 1079 *Journal of the Geological Society* **173**, 489–503.
20
21 1080
22
23 1081 Walsh, E. O., Hacker, B. R., Gans, P. B., Grove, M. & Gehrels, G. 2007. Protolith ages
24
25 1082 and exhumation histories of (ultra)high-pressure rocks across the Western Gneiss Region,
26
27 1083 Norway. *Journal of Metamorphic Geology* **119**, 289–301.
28
29 1084
30
31 1085 Walsh, E. O., Hacker, B. R., Gans, P. B., Wong, M. S. & Andersen, T. B. 2013. Crustal
32
33 1086 exhumation of the Western Gneiss Region UHP terrane, Norway: $^{40}\text{Ar}/^{39}\text{Ar}$
34
35 1087 thermochronology and fault-slip analysis. *Tectonophysics* **608**, 1159–1179.
36
37 1088
38
39 1089 Wiedenbeck, M., Allé, P., Corfu, F., Griffin, W. L., Meier, M., Oberli, F., von Quadt, A.,
40
41 1090 Roddick, J.C. & Spiegel, W. 1995. Three natural zircon standards for U-Th-Pb, Lu-Hf,
42
43 1091 trace element and REE analyses. *Geostandards Newsletter* **19**, 1–23.
44
45 1092
46
47
48
49
50
51
52
53
54
55
56
57
58
59
60

1
2
3 1093 Wilks, W. & Cuthbert, S. J. 1994. The evolution of the Hornelen Basin detachment
4
5 1094 system, western Norway: Implications for the style of late orogenic extension in the
6
7 1095 southern Scandinavian Caledonides. *Tectonophysics* **238**, 1-30.

9
10
11 1096

12
13 1097 Yakymchuk, C. & Brown, M. 2014. Behaviour of zircon and monazite during crustal
14
15 1098 melting. *Journal of the Geological Society London* **171**, 465-479.

16
17
18 1099

19
20 1100 Young, D. J. 2018. Structure of the (ultra)high-pressure Western Gneiss Region, Norway:
21
22 1101 Imbrication during Caledonian continental margin subduction. *GSA Bulletin* **130**, 926–94.

23
24
25 1102

26
27 1103 **Figure captions**

28
29 1104 Figure 1. (Colour online) (a) Simplified geological map of the Western Gneiss Region
30
31 1105 (modified after Brueckner & Cuthbert, 2013) with (b) generalised geological map of
32
33 1106 Fjortoft (after Carswell & van Roermund, 2005) showing the location of the diamond-
34
35 1107 bearing garnet kyanite gneiss. NSD - Nordfjord-Sogn detachment zone, MTD - Møre
36
37 1108 Trondelag detachment zone, black dashed line - early E/SE late W/NW décollements,
38
39 1109 black thin lines - W/NW vergent lineation directions.

40
41
42
43 1110

44
45 1111 Figure 2. (Colour online) Hand specimen of the diamond-bearing garnet-kyanite gneiss
46
47 1112 from Fjortoft (sample ID: Fj-19).

48
49
50 1113

51
52
53
54
55
56
57
58
59
60

1
2
3 1114 Figure 3. (Colour online) Cathodoluminescence images of representative zircon crystals
4
5 1115 from the Fjørtoft diamond-bearing garnet kyanite gneiss. White circles mark analytical
6
7 1116 spots and given numbers indicate ^{206}Pb - ^{238}U dates.
8
9

10 1117

11
12 1118 Figure 4. (Colour online) (a-d) U-Pb concordia diagram for zircon analyses; (a) all
13
14 1119 analyses for both metamorphic and detrital zircon domains, (b) concordia diagram of
15
16 1120 zircon with Caledonian ages with inset (c) showing ages for which Concordia age has
17
18 1121 been calculated. (d) Magnification of the fragment of Concordia diagram (a) showing late
19
20 1122 Precambrian dates. (e) Histogram of ^{206}Pb - ^{238}U age frequency of metamorphic zircon
21
22 1123 domains. (f) Histogram of ^{207}Pb - ^{206}Pb age frequency of concordant detrital zircon (10%
23
24 1124 discordance accepted).
25
26
27

28 1125
29
30
31
32
33
34
35
36
37
38
39
40
41
42
43
44
45
46
47
48
49
50
51
52
53
54
55
56
57
58
59
60

1126 Table 1. Summary of the U-Pb zircon analyses from the diamond-bearing garnet kyanite gneiss.

Analysis nr	U conc. (ppm)	Ratios						Common Pb		Degree of con- cordance (%)	Ages (Ma)						Comments	
		²⁰⁷ Pb/ ²⁰⁶ Pb	±2σ	²⁰⁷ Pb/ ²³⁵ U	±2σ	²⁰⁶ Pb/ ²³⁸ U	±2σ	rho:	²⁰⁶ Pb/ ²⁰⁴ Pb		f206%	²⁰⁶ Pb/ ²³⁸ U	±2σ	²⁰⁷ Pb/ ²³⁵ U	±2σ	²⁰⁷ Pb/ ²⁰⁶ Pb		±2σ
2	236	0.0558	0.0004	0.5454	0.0048	0.0709	0.0004	0.69	146049	0.01	99.6	441.7	2.6	442.0	3.2	443	14	rim
6	286	0.0554	0.0004	0.5195	0.0047	0.0680	0.0004	0.71	6482	0.27	98.8	424.0	2.6	424.8	3.1	429	14	metamorphic (no core)
17	384	0.0560	0.0003	0.5538	0.0056	0.0717	0.0006	0.79			98.7	446.5	3.5	447.5	3.7	452	14	rim
22	35	0.0555	0.0006	0.5348	0.0074	0.0699	0.0006	0.58	688	2.37	101.2	435.8	3.4	435.0	4.9	431	25	core
23	549	0.0553	0.0002	0.5219	0.0040	0.0685	0.0004	0.81	12869	0.13	100.6	426.8	2.6	426.4	2.7	424	10	rim
24	387	0.0552	0.0003	0.5191	0.0043	0.0682	0.0005	0.82	7163	0.23	101.1	425.3	2.8	424.6	2.9	421	11	core
25	106	0.0557	0.0004	0.5339	0.0049	0.0695	0.0004	0.69	2278	0.72	98.6	433.4	2.7	434.4	3.3	440	15	rim
27	125	0.0553	0.0004	0.5499	0.0051	0.0721	0.0005	0.72	26178	0.06	105.6	448.8	2.9	445.0	3.3	425	14	rim
28	30	0.0555	0.0008	0.5517	0.0089	0.0721	0.0005	0.47	2025	0.81	103.5	448.6	3.3	446.1	5.8	434	32	rim
30	233	0.0550	0.0003	0.5154	0.0042	0.0679	0.0004	0.74	2733	0.60	102.3	423.5	2.5	422.1	2.8	414	12	rim
31	207	0.0554	0.0002	0.5473	0.0054	0.0717	0.0006	0.89	22998	0.08	104.4	446.2	3.8	443.2	3.6	428	10	metamorphic (no core)
36	197	0.0553	0.0002	0.5332	0.0050	0.0699	0.0006	0.88	20051	0.09	102.8	435.8	3.4	433.9	3.3	424	10	metamorphic (no core)
37	211	0.0552	0.0002	0.5299	0.0048	0.0696	0.0006	0.90	6968	0.25	103.4	434.0	3.4	431.8	3.2	420	9	fragment of zircon grain
46	87	0.0562	0.0004	0.5574	0.0051	0.0719	0.0003	0.50			97.2	447.7	2.0	449.8	3.3	461	17	rim
52	307	0.0544	0.0003	0.4764	0.0036	0.0635	0.0003	0.55	356385	0.00	102.5	397.0	1.6	395.6	2.5	387	14	metamorphic (no core)
53	863	0.0553	0.0003	0.5192	0.0038	0.0681	0.0003	0.63			100.6	425.0	1.9	424.6	2.6	423	13	metamorphic (no core)
54	185	0.0561	0.0005	0.5540	0.0050	0.0716	0.0003	0.44			97.5	445.7	1.7	447.6	3.3	457	18	rim
55	839	0.0557	0.0004	0.5257	0.0061	0.0685	0.0006	0.81			97.1	427.0	3.9	429.0	4.0	440	15	core
61	182	0.0553	0.0002	0.5260	0.0044	0.0689	0.0005	0.87			100.8	429.7	3.0	429.2	2.9	426	9	metamorphic (no core)
62	265	0.0554	0.0002	0.5265	0.0031	0.0689	0.0003	0.83	15572	0.11	100.5	429.8	2.1	429.5	2.1	428	7	metamorphic (no core)
63	535	0.0553	0.0003	0.5171	0.0040	0.0678	0.0003	0.65	11250	0.16	99.4	422.8	2.1	423.2	2.7	425	13	fragment of zircon grain
64	189	0.0553	0.0002	0.5224	0.0031	0.0685	0.0003	0.78	2626	0.59	100.4	427.0	1.9	426.7	2.1	425	8	rim
65	81	0.0558	0.0004	0.5398	0.0048	0.0702	0.0003	0.52	1133	1.56	98.8	437.5	2.0	438.3	3.2	443	17	rim
67	160	0.0545	0.0005	0.5003	0.0056	0.0666	0.0004	0.53	3638	0.49	106.4	415.7	2.4	411.9	3.8	391	21	rim
71	249	0.0553	0.0002	0.5201	0.0040	0.0682	0.0004	0.86	6196	0.29	99.8	425.1	2.7	425.2	2.6	426	9	metamorphic (no core)
74	257	0.0554	0.0003	0.5264	0.0057	0.0689	0.0007	0.91	3931	0.42	100.1	429.5	4.1	429.4	3.8	429	10	rim
75	319	0.0554	0.0002	0.5258	0.0039	0.0688	0.0005	0.91			100.2	429.2	2.8	429.0	2.6	428	7	rim
78	157	0.0557	0.0003	0.5217	0.0041	0.0679	0.0004	0.78	2216	0.80	95.9	423.5	2.5	426.3	2.7	441	11	metamorphic (no core)
81	142	0.0556	0.0004	0.5335	0.0052	0.0696	0.0005	0.67	2456	0.72	99.3	433.7	2.8	434.1	3.5	437	16	metamorphic (no core)
96	250	0.0555	0.0004	0.5270	0.0044	0.0688	0.0004	0.61			98.9	429.0	2.1	429.8	2.9	434	15	metamorphic (no core)
97	385	0.0555	0.0004	0.5307	0.0044	0.0693	0.0003	0.60			99.8	432.2	2.1	432.3	2.9	433	15	core
101	147	0.0560	0.0003	0.5355	0.0047	0.0693	0.0005	0.74	3896	0.44	95.1	431.9	2.7	435.4	3.1	454	13	rim
102	233	0.0554	0.0003	0.5182	0.0041	0.0679	0.0004	0.70	103170	0.02	99.1	423.4	2.3	423.9	2.7	427	13	core
103	62	0.0554	0.0004	0.5233	0.0043	0.0685	0.0003	0.60	3546	0.46	99.5	427.0	2.0	427.4	2.9	429	15	metamorphic (no core)
104	223	0.0554	0.0003	0.5235	0.0040	0.0686	0.0004	0.71	20895	0.34	100.4	427.7	2.4	427.5	2.7	426	11	metamorphic (no core)
105	148	0.0559	0.0004	0.5068	0.0043	0.0658	0.0003	0.60			91.8	410.7	2.0	416.3	2.9	448	15	rim
60	78	0.0579	0.0005	0.6710	0.0061	0.0841	0.0003	0.43			99.2	520.6	2.0	521.3	3.7	525	18	rim
70	1362	0.0576	0.0001	0.6715	0.0040	0.0846	0.0005	0.94			101.8	523.4	2.9	521.6	2.5	514	4	core
69	118	0.0584	0.0004	0.7072	0.0063	0.0878	0.0005	0.58			99.4	542.5	2.7	543.1	3.8	546	16	rim
1	651	0.1042	0.0052	1.3385	0.0746	0.0932	0.0024	0.45	3766030	0.00	33.8	574.3	13.9	862.6	32.4	1700	92	core
5	261	0.0899	0.0005	3.3003	0.0281	0.2444	0.0017	0.77	53281	0.03	99.0	1409.5	9.0	1415.3	7.1	1424	11	core
7	251	0.2927	0.0021	16.1291	0.1504	0.3997	0.0023	0.62	9214	0.13	63.2	2167.4	10.7	2884.5	8.9	3432	11	core
12	191	0.1783	0.0010	12.5367	0.1365	0.5099	0.0048	0.86	43533	0.04	100.7	2656.0	20.5	2645.5	10.2	2637	9	core
13	128	0.0713	0.0004	1.6293	0.0273	0.1657	0.0026	0.94	3412	0.52	102.2	988.1	14.4	981.6	10.5	967	12	rim
14	1128	0.0653	0.0003	0.9729	0.0089	0.1081	0.0008	0.81	49091	0.04	84.6	661.9	4.7	690.0	4.6	783	11	core

1
2
3
4
5
6
7
8
9
10
11
12
13
14
15
16
17
18
19
20
21
22
23
24
25
26
27
28
29
30
31
32
33
34
35
36
37
38
39
40
41
42
43
44
45
46
47

15	206	0.0713	0.0003	1.4834	0.0124	0.1509	0.0010	0.81			93.8	905.9	5.7	923.6	5.1	966	10	rim
16	51	0.1677	0.0012	11.2274	0.2311	0.4855	0.0093	0.93	8352	0.21	100.6	2551.0	40.5	2542.2	19.2	2535	12	core
506	201	0.0830	0.0015	0.9346	0.0211	0.0817	0.0011	0.58	9400	0.17	39.9	506.2	6.4	670.0	11.1	1269	36	core
19	145	0.0651	0.0006	1.0268	0.0207	0.1145	0.0020	0.89	1246	1.31	90.0	698.7	11.9	717.3	10.4	776	19	core
743	658	0.0847	0.0006	1.4270	0.0231	0.1222	0.0018	0.90			56.8	743.3	10.3	900.3	9.7	1308	14	core
26	726	0.0760	0.0003	1.9710	0.0202	0.1882	0.0017	0.91	34372	0.05	101.6	1111.6	9.5	1105.7	6.9	1094	9	core
29	129	0.0700	0.0006	1.3920	0.0154	0.1442	0.0011	0.67	4447	0.37	93.5	868.2	6.0	885.5	6.5	929	17	core
35	960	0.0726	0.0006	1.6851	0.0318	0.1684	0.0029	0.91	20931	0.08	100.2	1003.5	15.9	1002.9	12.0	1002	16	core
39	573	0.1552	0.0013	4.9275	0.0732	0.2303	0.0028	0.82	10407	0.17	55.6	1335.9	14.8	1807.0	12.5	2404	14	core
40	485	0.1580	0.0012	4.9258	0.0798	0.2261	0.0033	0.89	52300	0.03	54.0	1314.0	17.1	1806.7	13.7	2434	13	core
42	935	0.0883	0.0006	2.1687	0.0343	0.1781	0.0025	0.89	19352	0.09	76.0	1056.3	13.8	1171.1	11.0	1390	14	core
43	442	0.0677	0.0005	1.3162	0.0186	0.1409	0.0017	0.84	15083	0.10	98.7	849.8	9.4	852.9	8.1	861	16	rim
45	605	0.0912	0.0006	3.1539	0.0372	0.2507	0.0024	0.82	27975	0.06	99.3	1442.1	12.5	1446.0	9.1	1452	13	core
48	371	0.0652	0.0009	1.2208	0.0202	0.1357	0.0012	0.52	7296	0.24	104.9	820.4	6.6	810.1	9.2	782	30	core
50	507	0.1488	0.0015	4.5197	0.0673	0.2204	0.0024	0.74	4529	0.31	55.1	1283.7	12.9	1734.6	12.4	2332	17	core
57	330	0.2115	0.0017	17.3921	0.2252	0.5963	0.0061	0.78			103.3	3014.9	24.5	2956.7	12.4	2917	13	core
59	435	0.1326	0.0033	5.8086	0.1765	0.3178	0.0056	0.58	14261	0.10	83.4	1778.8	27.2	1947.7	26.3	2132	43	core
66	279	0.1064	0.0003	2.9824	0.0428	0.2032	0.0029	0.98	18269	0.09	68.6	1192.5	15.3	1403.2	10.9	1739	5	core
68	965	0.0725	0.0003	1.6708	0.0146	0.1672	0.0013	0.91	29862	0.06	99.7	996.7	7.3	997.5	5.6	999	8	core
73	663	0.1576	0.0018	5.2052	0.1127	0.2395	0.0044	0.85	9696	0.18	56.9	1384.0	22.8	1853.5	18.4	2431	20	core
76	191	0.1777	0.0009	10.4769	0.1101	0.4275	0.0039	0.86	9230	0.19	87.2	2294.5	17.5	2477.9	9.7	2632	9	core
77	512	0.0666	0.0003	1.2174	0.0115	0.1326	0.0011	0.84			97.2	802.5	6.0	808.6	5.3	825	11	rim
80	655	0.1319	0.0009	3.1985	0.0376	0.1758	0.0017	0.82	253587	0.01	49.2	1044.2	9.2	1456.8	9.1	2124	12	rim
84	1089	0.1395	0.0012	4.2227	0.0793	0.2195	0.0037	0.89	30084	0.06	57.6	1279.2	19.4	1678.4	15.4	2221	15	core
86	269	0.1755	0.0011	11.2620	0.0972	0.4654	0.0028	0.70			94.3	2463.2	12.4	2545.1	8.0	2611	10	rim
87	153	0.1847	0.0011	12.4118	0.1241	0.4874	0.0038	0.78	9232	0.19	94.9	2559.3	16.6	2636.1	9.4	2696	10	core
88	151	0.1921	0.0012	14.0338	0.1553	0.5298	0.0049	0.84	19746	0.09	99.3	2740.4	20.7	2752.0	10.5	2761	10	core
91	33	0.1452	0.0015	3.2180	0.0506	0.1607	0.0019	0.74			41.9	960.6	10.4	1461.5	12.2	2291	18	core
92	25	0.1828	0.0014	8.2464	0.1310	0.3272	0.0046	0.88			68.1	1824.9	22.2	2258.4	14.4	2678	13	core
94	223	0.1197	0.0022	5.7115	0.1074	0.3462	0.0014	0.21			98.2	1916.4	6.6	1933.1	16.2	1951	33	core
95	37	0.0844	0.0006	2.5112	0.0225	0.2157	0.0012	0.64			96.7	1259.3	6.6	1275.3	6.5	1302	13	fragment of zircon grain
98	39	0.0637	0.0005	1.0104	0.0122	0.1150	0.0010	0.72	5605	0.31	95.8	701.7	5.8	709.1	6.1	733	18	rim
99	113	0.0689	0.0005	1.2650	0.0124	0.1333	0.0009	0.71			90.2	806.4	5.3	830.2	5.6	894	14	core
100	166	0.0658	0.0008	1.1848	0.0166	0.1306	0.0008	0.46	3066	0.56	98.8	791.0	4.8	793.5	7.7	801	26	rim
108	54	0.1390	0.0020	2.6482	0.0522	0.1381	0.0019	0.69	6571	0.26	37.7	834.1	10.6	1314.2	14.5	2215	25	core
110	194	0.1678	0.0017	8.0060	0.0934	0.3460	0.0021	0.53	4178964	0.00	75.5	1915.5	10.2	2231.7	10.5	2536	17	core

1127

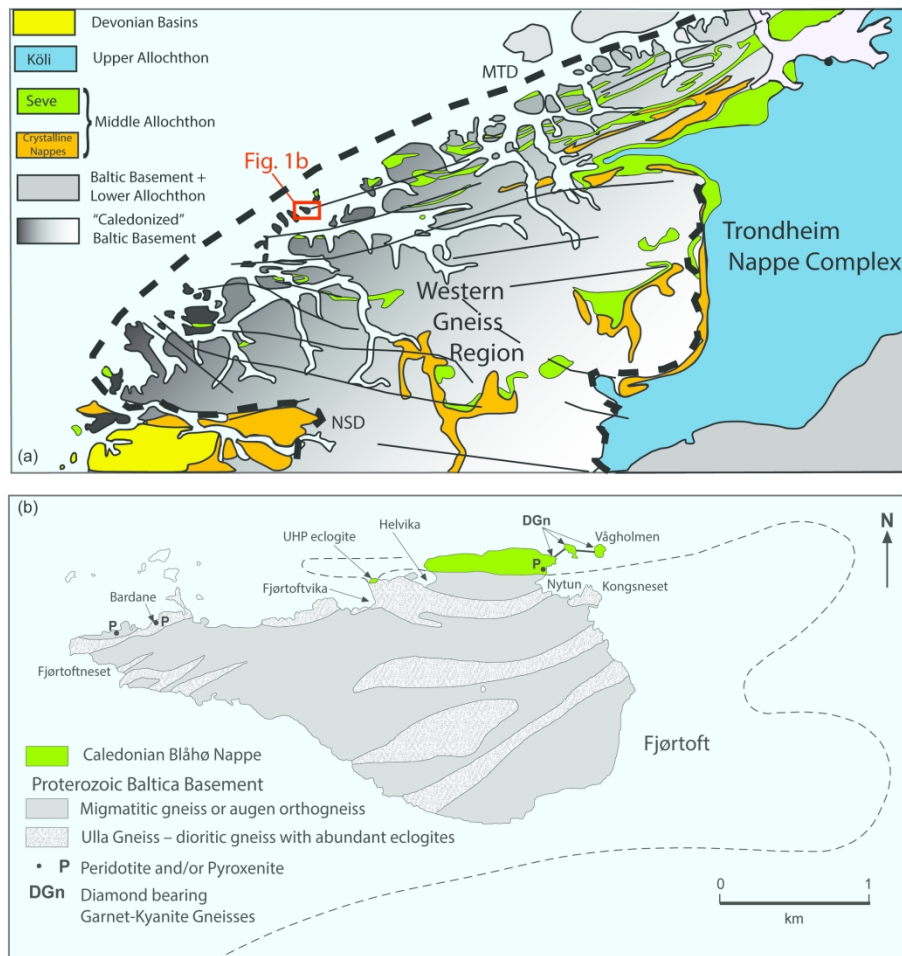


Figure 1. (Colour online) (a) Simplified geological map of the Western Gneiss Region (modified after Brueckner & Cuthbert, 2013) with (b) generalised geological map of Fjørtoft (after Carswell & van Roermund, 2005) showing the location of the diamond-bearing garnet kyanite gneiss. NSD - Nordfjord-Sogn detachment zone, MTD - Møre Trondelag detachment zone, black dashed line - early E/SE late W/NW décollements, black thin lines - W/NW vergent lineation directions.

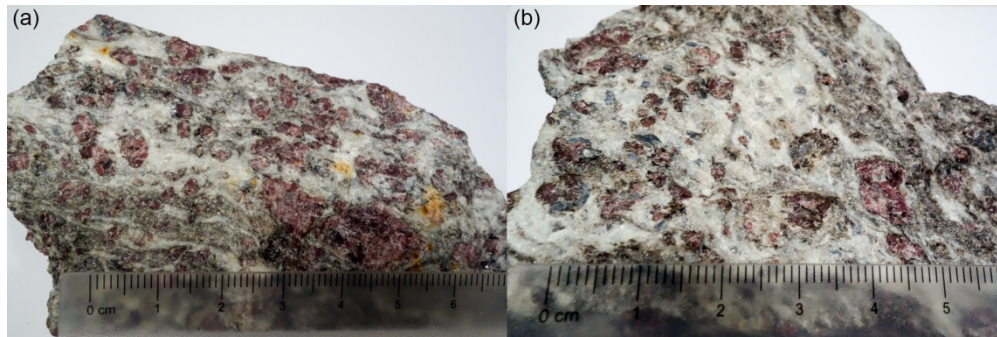
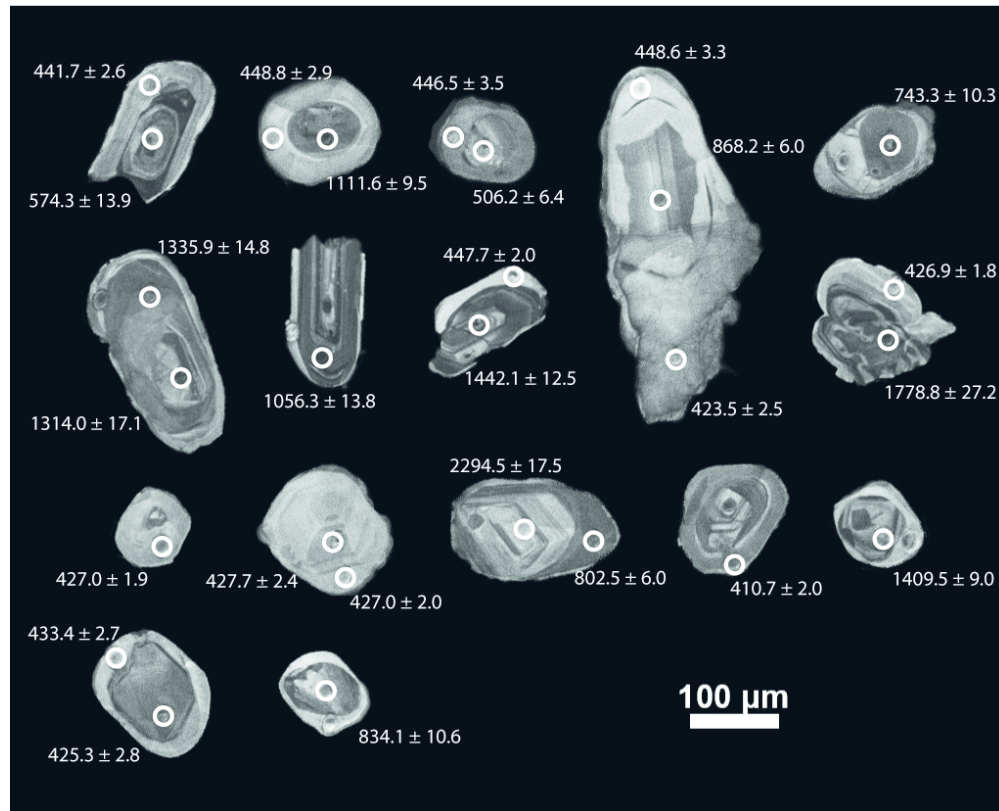


Figure 2. (Colour online) Hand specimen of the diamond-bearing garnet-kyanite gneiss from Fjørtoft (sample ID: Fj-19).



32
33
34
35
36
37
38
39
40
41
42
43
44
45
46
47
48
49
50
51
52
53
54
55
56
57
58
59
60

Figure 3. (Colour online) Cathodoluminescence images of representative zircon crystals from the Fjørtoft diamond-bearing garnet kyanite gneiss. White circles mark analytical spots and given numbers indicate ^{206}Pb - ^{238}U dates.

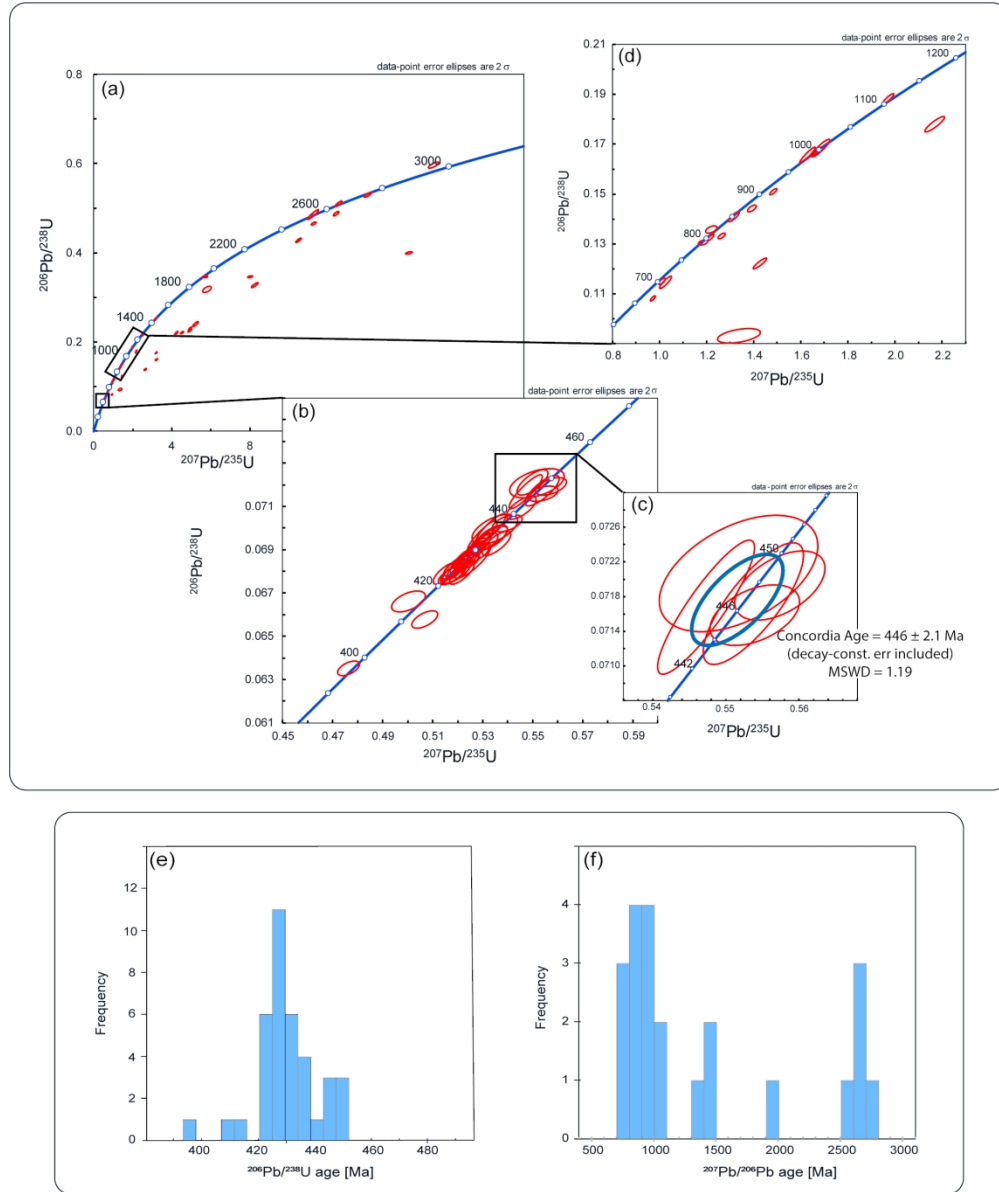


Figure 4. (Colour online) (a-d) U-Pb concordia diagram for zircon analyses; (a) all analyses for both metamorphic and detrital zircon domains, (b) concordia diagram of zircon with Caledonian ages with inset (c) showing ages for which Concordia age has been calculated. (d) Magnification of the fragment of Concordia diagram (a) showing late Precambrian dates. (e) Histogram of ^{206}Pb - ^{238}U age frequency of metamorphic zircon domains. (f) Histogram of ^{207}Pb - ^{206}Pb age frequency of concordant detrital zircon (10% discordance accepted).